An underwater photograph showing a large school of fish swimming in a blue ocean. A diver is visible in the center, surrounded by the fish. The scene is captured from a low angle, looking up towards the surface.

Synchronization of Uncertain Heterogeneous Agents: An Adaptive Virtual Model Reference Approach

Muhammad Ridho Rosa

Master of Science Thesis

Synchronization of Uncertain Heterogeneous Agents: An Adaptive Virtual Model Reference Approach

MASTER OF SCIENCE THESIS

For the degree of Master of Science in Embedded Systems at Delft
University of Technology

Muhammad Ridho Rosa

July 1, 2018

Faculty of Electrical Engineering, Mathematics and Computer Science · Delft
University of Technology

DELFT UNIVERSITY OF TECHNOLOGY
DEPARTMENT OF
DELFT CENTER FOR SYSTEMS AND CONTROL (DCSC)

The undersigned hereby certify that they have read the master of science thesis
report

SYNCHRONIZATION OF UNCERTAIN HETEROGENEOUS AGENTS: AN ADAPTIVE
VIRTUAL MODEL REFERENCE APPROACH

by

MUHAMMAD RIDHO ROSA
MASTER OF SCIENCE EMBEDDED SYSTEMS

Dated: July 1, 2018

Supervisor(s):

Dr. Simone Baldi

Reader(s):

Dr. ir. T.J.J van den Boom

Dr. ir. Arjan van Genderen

Dr. Sander Wahls

Abstract

Synchronization of Multi-Agent Systems (MASs) has the potential to benefit many technological areas such as formation control for unmanned vehicles, cooperative adaptive cruise control, and spacecraft attitude control. Information plays a crucial role in MASs: in centralized approaches, a central node utilizes global information to achieve synchronization, while in distributed approach agents only utilize local information, i.e. neighbors' information. A big concern in MASs is the presence of parametric uncertainties (unknown dynamics), which might require adaptive control gains instead of fixed control gains.

This work thus provides a novel adaptive distributed control for MASs of heterogeneous agents with unknown dynamics based on model reference adaptive control (MRAC). We study both the synchronization of linear systems and the synchronization of Euler-Lagrange (EL) systems. The implementation of this scheme is based on distributed matching condition assumptions. We study such matching conditions both for the state-feedback case and output-feedback case. Since all matching gains are unknown in view of the unknown dynamics, the gains are adapted online via Lyapunov-based estimation. The asymptotic convergence of the synchronization error is analytically proven by introducing an appropriately defined Lyapunov function, and numerical examples show the effectiveness of the approach. The practical advantage of the proposed distributed MRAC is the possibility of handling unknown dynamics by simply exchanging the states/output, and inputs with neighbors, without any extra auxiliary variables (distributed observer) nor sliding mode. Because of the mutual dependence of control inputs, well-posedness problems will arise in the presence of cyclic communication, if the inputs are generated without a prescribed priority. In this work, we study such well-posedness problems via parameter projection methods.

Contents

1	Introduction	11
1-1	Synchronization of multi-agent systems	11
1-2	State of the art	12
1-3	Research objective	13
1-4	Report outline	14
2	Adaptive synchronization of uncertain linear systems	15
2-1	Communication graph	15
2-2	State-feedback MRAC	16
2-2-1	Synchronization of a leader to a reference model	17
2-2-2	Synchronization of a follower to a neighbor	19
2-2-3	Synchronization of a follower to two neighbors	21
2-2-4	Extension to acyclic graphs	23
2-3	Output-feedback MRAC	24
2-3-1	Synchronization of a leader to a reference model	26
2-3-2	Synchronization of a follower to a neighbor	29
2-3-3	Synchronization of a follower to two neighbors	32
2-3-4	Extension to acyclic graphs	34
2-3-5	Summary	36
3	Adaptive synchronization with cyclic communication network	37
3-1	Well-posedness of the input	37
3-2	Summary	41

4	Adaptive synchronization of uncertain Euler-Lagrange system	43
4-1	Preliminaries results	43
4-1-1	Euler-Lagrange systems	43
4-1-2	Inverse dynamic based control	44
4-2	Adaptive synchronization of a leader to a reference model	45
4-3	Adaptive synchronization of a follower to a neighbor	48
4-3-1	Extension to acyclic graphs	52
4-3-2	Summary	54
5	Numerical simulations	55
5-1	Output-feedback MRAC: Yaw attitude control of multi UAV	55
5-2	Cyclic state-feedback MRAC: Platooning merging maneuver	60
5-3	Euler-Lagrange systems MRAC: Formation control for multi-aircraft systems .	64
6	Conclusion and future work	69
6-1	Conclusion	69
6-2	Future work	70
	Bibliography	71

List of Figures

2-1	Multi-agent system communication graph.	16
2-2	A leader-follower communication graph with one follower (state-feedback). .	17
2-3	A leader-follower communication graph with two followers (state-feedback). .	21
2-4	A leader-follower communication graph with one follower (output-feedback). .	25
2-5	A leader-follower directed communication graph with two followers (output-feedback).	32
3-1	A communication graph with a cycle	38
3-2	Singular set (red curve) and projection set (shaded blue area)	39
4-1	Example of multi-agent system communication graph for EL systems.	45
5-1	The switching adaptive control for agent k	56
5-2	The directed communication graph output-feedback scheme with switching topology.	57
5-3	Switching edge σ	58
5-4	Output response of the output-feedback MRAC with a constant input reference where the controller is not switching (a) and the controller is switching (b).	59
5-5	Output response of the output-feedback MRAC with a sinusoidal input reference where the controller is not switching (a) and the controller is switching (b).	59
5-6	The communication graphs before, during and after merging (Platooning Merging Maneuver Case)	61
5-7	The position response (Platooning Merging Maneuver Case)	62

5-8	The velocity response (Platooning Merging Maneuver Case)	63
5-9	The acceleration response (Platooning Merging Maneuver Case)	63
5-10	The input response (Platooning Merging Maneuver Case)	63
5-11	Adaptive state synchronization for states $(x, y, z, \bar{u}, \bar{v}, \bar{w})$ (Synchronization of Multi-Aircraft System)	65
5-12	Adaptive state synchronization for states $(\phi, \theta, \psi, \bar{p}, \bar{q}, \bar{r})$ (Synchronization of Multi-Aircraft System)	66
5-13	Adaptive state synchronization in the inertial xy plane without formation gaps (Synchronization of Multi-Aircraft System)	66
5-14	Adaptive formation control in the inertial xy plane for V formation flight (Synchronization of Multi-Aircraft System)	67

List of Tables

5-1	Quadcopter parameters and initial conditions.	57
5-2	Vehicles parameters and initial conditions	62
5-3	Fixed-wing UAVs parameters and initial conditions	65

List of Notation

The notations used in the MSc thesis are

\mathbb{G} : the directed graph which consists of a pair $(\mathcal{N}, \mathcal{E})$.

\mathcal{N} : a set of nodes $\mathcal{N} = \{1, \dots, n\}$.

\mathcal{E} : a set of edges $\mathcal{E} \subseteq \mathcal{N} \times \mathcal{N}$.

a_{ij} : the edge's weight where $i \neq j$.

\mathbb{R} : the set of real numbers.

\mathbb{P} : the projection operator.

Capital letter (e.g., P): used for matrices.

$P = P^T > 0$: a symmetric positive definite matrix.

\mathbb{I} : the identity matrix of compatible dimensions.

$\text{diag } \{\dots\}$: a block-diagonal matrix.

$\text{sgn}(\bullet)$: the sign of \bullet .

Small letter (e.g., x): used for vectors.

\mathcal{L}_2 class: A vector signal $x \in \mathbb{R}^n$ belongs to the \mathcal{L}_2 class; if $\int_0^t \|x(\tau)\|^2 d\tau < \infty$, $\forall t > 0$.

\mathcal{L}_∞ class: A vector signal $x \in \mathbb{R}^n$ belongs to \mathcal{L}_∞ class; if $\max \|x(t)\| < \infty$, $\forall t > 0$.

Acknowledgment

First and foremost, I would like to express my deepest gratitude to my supervisor, Dr. ir. Simone Baldi, for giving me the opportunity to work on a very interesting topic. He has patiently guided me to develop my research skill through his supervision and discussions.

I would also like to thank the government of Indonesia, especially LPDP for supporting me during my two-year study in TU Delft. Huge thanks to ESCEndOL (Embedded System, Computer Engineering, and System Control) group for the serious discussions and relaxing moments during our study in the Netherlands, and my thanks also go to PPI Delft for making the Netherlands feels like home. Many thanks to everyone that directly or indirectly helped me to finish this thesis.

Finally, I am grateful to my wife for sharing ups and downs, and my parents for their support and trust.

Delft, University of Technology
July 1, 2018

Muhammad Ridho Rosa

Chapter 1

Introduction

Synchronization of the multi-agent system (MASs) is an active area of research with many exciting applications. The implementation of a control law that can adapt to parameter uncertainties and has the capability to handle time-varying communication graph is crucial in the implementation. Although, some research has been done, only limited classes of uncertainty that has been addressed. In this chapter, we introduce the synchronization problem of MASs to handle heterogeneous systems with unknown dynamics.

This chapter is organized as follows: Section 1-1 introduces the MASs and the synchronization of MASs where the adaptive approach has not been proposed. Section 1-2 presents the state of art methodologies that have been proposed in this field to address the parameter uncertainties and the unknown dynamics of the agents. Section 1-3 summarizes the research objectives of this MSc thesis. Finally, Section 1-4 concludes this chapter by presenting the outline of MSc thesis report.

1-1 Synchronization of multi-agent systems

In recent years, the synchronization of MASs has been an emerging research direction drawing the attention of the control community. Synchronization represents a potential solution for coordination of large-scale networked systems [1,2], encompassing spacecraft attitude control [3], sensor networks [4], smart buildings and smart grids [5–7], unmanned aerial, ground and underwater vehicles [8–10].

Prior to an explanation of the theory of synchronization of MASs, it is useful to give a definition of "agent". The term "agent" appears in multiple disciplines in engineering and science; therefore, the term has been continuously revised. According to [11], an

agent consists of four basic elements: the sensor, the actuator, the information element, and the reasoning element. According to [12], agents can be divided into three main categories: human agents, hardware agents, and software agents. Depending on the task, the software agent can be broken down into information agents, cooperation agents, and transaction agents.

To coordinate MASs, either a centralized approach or a distributed approach can be adopted. The centralized approach introduces a central node that utilizes the information stemming from all agents to control them. On the contrary, the distributed approach uses, for each agent, a controller that utilizes local information, i.e. neighbors' information. The distributed approach gives more advantages due to its applicability in the presence of communication constraints [13–15]. The research direction in distributed control can be grouped into several directions that may be overlapping, such as synchronization (sometimes referred to as consensus or rendezvous when the synchronizing behavior is constant), distributed formation control (sometimes referred to as flocking in the presence of collision avoidance capabilities), distributed optimization and estimation [16].

Based on the existence of the leader agent, the synchronization could be divided into two types of synchronization, leaderless synchronization and leader-follower synchronization. In this work, we will only discuss the leader-follower synchronization. Here, the agents have the objective to synchronize to the leader dynamics where the error between the agents and the leader converge asymptotically to zero. In general, the study of synchronization has the objective of finding the coupling gains and the network topology that guarantee the synchronization state error or the synchronization output error converges asymptotically to zero. Initial research on synchronization has been focusing on networks of identical agents, e.g., [17,18]. However, it is well known that agents can have heterogeneous dynamics, which makes synchronization more challenging [19,20]. Fixed coupling gains among the identical and non-identical agents that stabilize the synchronization error and guarantee the desired performance were proposed in [21,22]. Currently, the cooperative regulation under large uncertainties or unknown dynamics has not been discussed widely. Therefore, the adaptive-gain distributed control is necessary to handle the heterogeneous agent with unknown dynamics. Note that the previous works were using the global information, the eigenvalues of the Laplacian matrix (algebraic connectivity), that will be excluded in this thesis.

1-2 State of the art

The design of the adaptive distributed controller is utmost importance on dealing with large uncertainties. Several methods of the adaptive distributed controller that has been proposed are the adaptive distributed control based on passification method and the adaptive distributed control based on model reference adaptive control (MRAC). In passification method, a distributed observer of the exogenous signal and a reference

model whose output can converge to the exogenous signal are designed to synchronize the agents. The passification method was used to design the adaptive distributed controller and solve the problem for the output regulation was proposed in [23, 24]. It is known that the passification method provides less restrictive matching conditions based on regulator equations for tracking a given class of exogenous signals compared to state-feedback MRAC approach [25]. However, the passification method assumes that every agent knows the matrix of the exosystem.

The adaptive distributed control based on state-feedback MRAC was proved to synchronize the heterogeneous agent with unknown dynamics via strict matching condition and adaptive laws [25]. In that work, synchronization was reached by using an extended form of state feedback model reference adaptive control (MRAC) where the vector coupling gains are used. Based on that research, we provide less restrictive matching condition by introducing the extension of output-feedback MRAC. The extension of output-feedback MRAC assumes the relative degree of a linear system is the same as the reference model. Then, we extend the capability to handle the switching topologies by introducing multiple switched controller. We proposed the switched controller based on the number of the agent predecessors where the learning process should be held whenever the controller inactive. It is widely known that there exist stability analysis of switched system based on dwell time analysis [26, 27]. All the works as mentioned earlier based on MRAC approach rely on the directed acyclic graph (DAG) assumption. However, for some certain purposes (i.e., merging maneuvers) having the undirected graph or directed graph with a cycle is necessary. Therefore, we propose a well-posedness of the input that is designed to handle the synchronization under undirected graph or directed graph with a cycle. Furthermore, we extend our work to synchronize the Euler-Lagrange (EL) systems, which use state-feedback MRAC and inverse dynamic based control. Two things shown in these works must be remarked: first, exchanging the inputs makes any exchange of auxiliary variables unnecessary, resulting overall in less communication effort (because the input to be exchanged has typically a smaller dimension than the observer variables); second, arbitrarily time-varying leader trajectories can be handled without requiring any global knowledge of such trajectory neither any sliding mode.

1-3 Research objective

The synchronization of MASs reveals the need for adaptive control approach which can handle the uncertainties and the unknown agent's dynamics. The extension of state-feedback MRAC has been used to synchronize the agents with unknown dynamics. Thus, the output-feedback MRAC focusing on the problem of cooperative output regulation in the presence of the uncertainties and the unknown agent's dynamics is necessary. The graph communication with a cycle is obligatory to perform merging maneuvers. It is known that the EL systems can be employed to describe a wide class of practical systems. Thus we propose the adaptive hierarchical control for uncertain EL systems using distributed inverse dynamics. Consequently, the research objectives throughout

this MSC thesis are defined:

- Synchronization of linear systems (output-feedback MRAC): Design the adaptive control law based on output-feedback MRAC where only local information (agent's input and agent's output) are required to synchronize all the agents.
- Undirected graph and the cycle: Presents the condition that is satisfied the synchronization under undirected graph and directed graph with a cycle.
- Synchronization of EL systems: Design the distributed adaptive control law for uncertain heterogeneous nonlinear agent described by EL systems.

1-4 Report outline

The rest of the MSc thesis report is organized as follows:

- **Chapter 2** introduces state-feedback and output-feedback synchronization based on the distributed MRAC approach.
- **Chapter 3** studies the well-posedness of the input under undirected graph and graph with cycles.
- **Chapter 4** introduces synchronization of EL systems based on distributed inverse dynamics and MRAC.
- **Chapter 5** presents the numerical simulations used to validate the theoretical findings.
- **Chapter 6** provides conclusions and proposes directions for further research.

Chapter 2

Adaptive synchronization of uncertain linear systems

This chapter is organized as follows: Section 2-1 introduces the communication graph in general. Section 2-2 presents the previous work of synchronization of MASs based on state-feedback MRAC. Section 2-3 extends the output-feedback MRAC to handle the synchronization of MASs with unknown dynamics.

2-1 Communication graph

In this work, we consider networks of agents (linear systems or EL systems) which are linked to each other via a communication graph that describes the allowed information flow. In other words, we say that system i has a *directed* connection to system j if the second can receive information from the first. Here, informations are states x_i, q_i, \dot{q}_i or output (y_i) measurements and input measurements u_i, τ_i from neighbors. In a communication graph, a special role is played by the *pinning* node, which is an agent (typically indicated as system 0) that does not receive information from any other agents in the network. Note that the pinner can be a virtual or a real agent, depending on the particular application. The communication graph describing the allowed information flow between all the systems, pinner excluded, is completely defined by the pair $\mathcal{G} = (\mathcal{V}, \mathcal{E})$, where $\mathcal{V} = \{1, \dots, N\}$ is a finite nonempty set of nodes, and $\mathcal{E} \subseteq \mathcal{V} \times \mathcal{V}$ is a set of pairs of nodes, called edges. To include the presence of the pinner in the network we define $\bar{\mathcal{G}} = \{\mathcal{V}, \mathcal{E}, \mathcal{T}\}$, where $\mathcal{T} \subseteq \mathcal{V}$ is the set of those nodes, called *target nodes*, which receive information from the pinner.

Figure 2-1 provides a simple communication graph where $\mathcal{V} = \{1, 2, 3, \}$, $\mathcal{E} = \{(1, 2), (1, 3)\}$, and $\mathcal{T} = \{1, \}$. Note that the target node will be referred to as a leader in this work

because they can access the information of the pinner: with this directed connection, follower 3 can observe the measurement from leader 1 and follower 2, but not vice versa. Let us introduce the *adjacency matrix* $\mathcal{A} = [a_{ij}] \in \mathbb{R}^{N \times N}$ of a directed communication

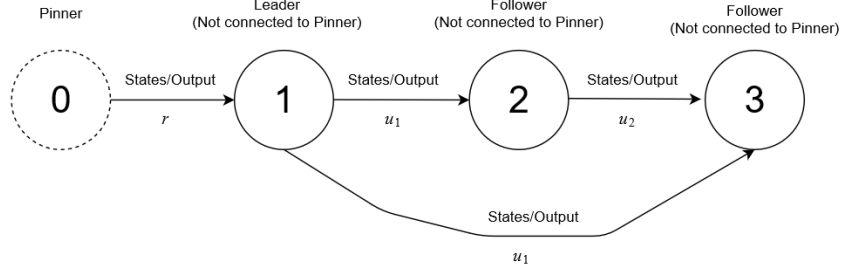


Figure 2-1: Multi-agent system communication graph.

graph, which is defined as $a_{ii} = 0$ and $a_{ij} = 1$ if $(i, j) \in \mathcal{E}$, where $i \neq j$. The adjacency matrix corresponding to the example in Figure 2-1 is

$$\mathcal{A} = \begin{bmatrix} 0 & 1 & 1 \\ 0 & 0 & 1 \\ 0 & 0 & 0 \end{bmatrix}.$$

In addition, we define a vector, the *target vector* $\mathcal{M} = [a_{j0}] \in \mathbb{R}^N$, to describe the directed communication of the pinner with the target nodes. Specifically, the target matrix is defined as $a_{j0} = 1$ if $j \in \mathcal{T}$ and $a_{j0} = 0$ otherwise. In the example of Figure 2-1, we have $\mathcal{M} = [1, 0, 0]'$. A directed graph $\bar{\mathcal{G}}$ is said to be *hierarchical* if the vertices of the graph can be sorted in such a way that the adjacency matrix has upper triangular form with only zeros in the diagonal, which is the case of the graph in Figure 2-1: this is equivalent to saying that the directed communication graph is acyclic (in Chapter 3 we discuss the Cyclic case). Also, the graph is said to contain a *directed spanning tree* with the pinner as the root node, if for every agent j there is a directed path that leads from j to 0. In this chapter we will consider acyclic networks containing a directed spanning tree with the pinner as the root node. Considering acyclic networks is a necessary consequence of exchanging control inputs among neighbors, because the mutual dependence of control inputs will bring well-posedness problems if the inputs are generated without a prescribed priority [28]; however, it was shown in [29] that the distributed model reference adaptive framework can work, with appropriate modifications, also in the presence of cyclic networks.

2-2 State-feedback MRAC

In line with [25], the objective in this section is to find the control laws u for each agent that guarantee synchronization of MASs with unknown linear dynamics by only using

the input and the states of the neighbors. First, let us assume that there are three agents denoted with subscripts 0, 1, and 2. Let us consider the network depicted in Figure 2-2. Here, the purpose of agent 1, the leader, is to follow agent 0. At the same time, the purpose of agent 2 is to follow agent 1. agent 0 is a reference model that is connected to agent 1, satisfying the following dynamics:

$$\dot{x}_m = A_m x_m + b_m r \quad (2-1)$$

where $x_m \in \mathbb{R}^n$ is the state of the reference model, $r \in \mathbb{R}$ is the reference input of the reference model. A_m and b_m are known matrices of appropriate dimensions. Then to have a bounded state trajectory x_m for bounded r , A_m should be Hurwitz. Then, we have agents 1 and 2, denoted with subscripts 1 and 2, respectively, and with dynamics expressed in the following dynamics

$$\dot{x}_1 = A_1 x_1 + b_1 u_1 \quad (2-2)$$

$$\dot{x}_2 = A_2 x_2 + b_2 u_2 \quad (2-3)$$

where $x_1, x_2 \in \mathbb{R}^n$ is the state, $u_1, u_2 \in \mathbb{R}$ is the inputs. Then we have A_1, A_2 and b_1, b_2 are unknown matrices of appropriate dimensions, with possibly $A_1 \neq A_2$ and $b_1 \neq b_2$ (heterogeneous unknown agents). We assume a directed connection from agent 1 to agent 2, i.e., the digraph is described by $\mathcal{N} = \{1, 2\}$, $\mathcal{E} = \{(1, 2)\}$. By using this configuration, agent 2 can observe the measurement from agent 1, but not vice versa.

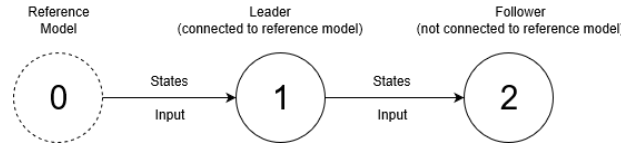


Figure 2-2: A leader-follower communication graph with one follower (state-feedback).

2-2-1 Synchronization of a leader to a reference model

Applying classical model reference adaptive control, it is known that agent 1 can synchronize to the reference model (2-1) through the controller

$$u_1(t) = k_1^{*'} x_1(t) + l_1^* r(t) \quad (2-4)$$

where $k_1^{*'}$, l_1^* are the optimum feedback gains that should be satisfied the following assumptions.

Assumption 1. There exist constant vectors k_1^*, k_2^* and scalars l_1^*, l_2^* such that

$$\begin{aligned} A_m &= A_1 + b_1 k_1^{*'}, & b_m &= b_1 l_1^* \\ A_m &= A_2 + b_2 k_2^{*'}, & b_m &= b_2 l_2^*. \end{aligned} \quad (2-5)$$

Assumption 2. The sign of l_1^*, l_2^* are known.

Remark 1. Assumptions 1 and 2 are standard in state-feedback MRAC [30, Chapter 5], so that we can adopt the same assumptions also in the setting of adaptive synchronization of MASs.

Being the system matrices (2-2) unknown, the proposed control law (2-4) cannot be implemented for agent 1, then we can come up with

$$u_1(t) = k_1'(t)x_1(t) + l_1(t)r(t) \quad (2-6)$$

where k_1', l_1 are estimates of k_1^*, l_1^* respectively. Let us define the error $e_1 = x_1 - x_m$, whose dynamics are

$$\dot{e}_1(t) = A_m e_1(t) + b_1(\tilde{k}_1'(t)x_1(t) + \tilde{l}_1(t)r(t)) \quad (2-7)$$

where $\tilde{k}_1' = k_1 - k_1^*$, $\tilde{l}_1 = l_1 - l_1^*$. The following result is basically standard state-feedback MRAC.

Theorem 1. Consider the reference model (2-1), the unknown leader dynamics (2-2), the controller (2-6), and the adaptive laws

$$\begin{aligned} \dot{k}_1'(t) &= -\text{sgn}(l_1^*)\gamma b_m' P(x_1(t) - x_m(t))x_1(t)' \\ \dot{l}_1'(t) &= -\text{sgn}(l_1^*)\gamma b_m' P(x_1(t) - x_m(t))r(t) \end{aligned} \quad (2-8)$$

where the scalar $\gamma > 0$ is the adaptive gain, and P is a positive definite matrix satisfying

$$PA_m + A_m'P = -Q, \quad Q > 0 \quad (2-9)$$

then we guarantee synchronization of the leader dynamics(2-2) to the reference model (2-1), and the convergence $e_1 \rightarrow 0$ for $t \rightarrow \infty$.

Proof. To analytically show the asymptotic convergence of the synchronization error between the leader and the reference model, one can introduce the following Lyapunov function

$$V_1(e_1, \tilde{k}_1, \tilde{l}_1) = e_1' P e_1 + \text{tr}\left(\frac{\tilde{k}_1' \tilde{k}_1}{\gamma |l_1^*|}\right) + \frac{\tilde{l}_1^2}{\gamma |l_1^*|}. \quad (2-10)$$

Then it is possible to verify

$$\begin{aligned} \dot{V}_1 &= e_1'(PA_m + A_m'P)e_1 + 2e_1'Pb_1(\tilde{k}_1'x_1 + \tilde{l}_1r) + 2\text{tr}\left(\frac{\tilde{k}_1'\gamma^{-1}\dot{\tilde{k}}_1}{|l_1^*|}\right) + 2\frac{\tilde{l}_1\gamma^{-1}\dot{\tilde{l}}_1}{|l_1^*|} \\ &= -e_1'Qe_1 + 2(\text{sgn}(l_1^*)b_m'P(x_1 - x_m)x_1' + \gamma^{-1}\dot{\tilde{k}}_1')\frac{\tilde{k}_1}{|l_1^*|} \\ &\quad + 2(\text{sgn}(l_1^*)b_m'P(x_1 - x_m)r + \gamma^{-1}\dot{\tilde{l}}_1)\frac{\tilde{l}_1}{|l_1^*|} \\ &= -e_1'Qe_1. \end{aligned} \quad (2-11)$$

From (2-11), we obtain that V_1 has a finite limit, so $e_1, \tilde{k}_1, \tilde{l}_1 \in \mathcal{L}_\infty$. Because $e_1 \in \mathcal{L}_\infty$ and $x_m \in \mathcal{L}_\infty$, we have $x_1 \in \mathcal{L}_\infty$. This implies $k_1', l_1 \in \mathcal{L}_\infty$. We have controller (2-6) and $k_1', l_1 \in \mathcal{L}_\infty$, so that we have $u_1 \in \mathcal{L}_\infty$. Therefore, all signals in the closed-loop system are bounded. From (2-11), we can establish that \dot{V}_1 has a bounded integral, so we have $e_1 \in \mathcal{L}_2$. This implies $\dot{V}_1 \rightarrow 0$ for $t \rightarrow \infty$ hence $e_1 \rightarrow 0$ for $t \rightarrow \infty$, which concludes the proof. \square

Remark 2. Note that Theorem 1 requires the agent to obtain the reference signal r to synchronize to its neighbors which is not possible in a distributed setting. Therefore, the signals of neighboring agents will be utilized instead of the reference signal.

2-2-2 Synchronization of a follower to a neighbor

In this subsection, we will design an adaptive control that can synchronize agent 2 to agent 1 without using the reference input and reference states. In known parameter case, one can have the control law for agent 2 as follows

$$u_2(t) = k_{21}^{*'}(t)x_1(t) + k_2^{*'}(t)(x_2(t) - x_1(t)) + l_{21}^*(t)u_1(t). \quad (2-12)$$

The following proposition is the result of Assumption 1.

Proposition 1. There exist a constant vector k_{21}^* and a scalar l_{21}^* such that

$$A_1 = A_2 + b_2 k_{21}^{*'}, \quad b_1 = b_2 l_{21}^*. \quad (2-13)$$

It implies that agent 2 can match agent 1 via k_{21}^* and l_{21}^* , which we refer to as coupling gains.

Proof. Let us consider the equation (2-5), then we can come up with

$$\begin{aligned} b_1 &= b_2 \frac{l_2^*}{l_1^*} \\ A_1 - A_2 &= b_2 k_2^{*'} - b_1 k_1^{*'} \\ &= b_2 \left[k_2^{*'} - \frac{l_2^*}{l_1^*} k_1^{*'} \right] \end{aligned} \quad (2-14)$$

which is in the form of (2-13) we have $k_{21}^{*'} = k_2^{*'} - \frac{l_2^*}{l_1^*} k_1^{*'}$, and $l_{21}^{*'} = \frac{l_2^*}{l_1^*}$. \square

Remark 3. Proposition 1 shows us a distributed matching condition among neighboring agents in synchronization of MASs (state-feedback case). In other words, there exist coupling gains that match an agent to its neighbors. Such distributed matching condition has been derived without extra assumptions than the standard assumptions of adaptive control.

Being the system matrices (2-3) unknown, the proposed control law (2-12) cannot be implemented for agent 2. Then we propose the control law

$$u_2(t) = k'_{21}(t)x_1(t) + k'_2(t)(x_2(t) - x_1(t)) + l_{21}(t)u_1(t) \quad (2-15)$$

where k'_{21} , k'_2 , l_{21} are the estimates of k^*_{21} , k^*_2 , l^*_{21} respectively. Let us define the error $e_{21} = x_2 - x_1$, whose dynamics are

$$\dot{e}_{21}(t) = A_m e_{21}(t) + b_2(\tilde{k}'_{21}(t)x_1(t) + \tilde{k}'_2 e_{21} + \tilde{l}_{21}u_1(t)) \quad (2-16)$$

where $\tilde{k}'_{21} = k_{21} - k^*_{21}$, $\tilde{k}'_2 = k_2 - k^*_2$, $\tilde{l}_{21} = l_{21} - l^*_{21}$. The following Theorem provides the leader-follower synchronization.

Theorem 2. Consider the unknown leader dynamics (2-3), the unknown follower dynamics (2-3), the controller (2-15), and the adaptive laws

$$\begin{aligned} \dot{k}'_{21}(t) &= -\text{sgn}(l_2^*)\gamma b'_m P(x_2(t) - x_1(t))x_1(t)' \\ \dot{k}'_2(t) &= -\text{sgn}(l_2^*)\gamma b'_m P(x_2(t) - x_1(t))(x_2(t) - x_1(t))' \\ \dot{l}_{21}(t) &= -\text{sgn}(l_2^*)\gamma b'_m P(x_2(t) - x_1(t))u_1(t) \end{aligned} \quad (2-17)$$

then we guarantee synchronization of the follower dynamics(2-3) to the leader dynamics (2-2), and the convergence $e_{21} \rightarrow 0$ for $t \rightarrow \infty$.

Proof. To analytically show the asymptotic convergence of the synchronization error between the follower and the leader, one can introduce the following Lyapunov function

$$V_{21}(e_{21}, \tilde{k}_{21}, \tilde{k}_2, \tilde{l}_{21}) = e'_{21} P e_{21} + \text{tr}\left(\frac{\tilde{k}'_{21} \tilde{k}_{21}}{\gamma |l_2^*|}\right) + \text{tr}\left(\frac{\tilde{k}'_2 \tilde{k}_2}{\gamma |l_2^*|}\right) + \frac{\tilde{l}_{21}^2}{\gamma |l_2^*|}. \quad (2-18)$$

Then it is possible to verify

$$\begin{aligned} \dot{V}_{21} &= e'_{21}(P A_m + A'_m P) e_{21} + 2e'_{21} P b_2(\tilde{k}'_{21} x_1 + \tilde{k}'_2 e_{21} + \tilde{l}_{21} u_1) + 2\text{tr}\left(\frac{\tilde{k}'_{21} \gamma^{-1} \dot{\tilde{k}}_{21}}{|l_2^*|}\right) \\ &\quad + 2\text{tr}\left(\frac{\tilde{k}'_2 \gamma^{-1} \dot{\tilde{k}}_2}{|l_2^*|}\right) + 2\frac{\tilde{l}_{21} \gamma^{-1} \dot{\tilde{l}}_{21}}{|l_2^*|} \\ &= -e'_{21} Q e_{21} + 2(\text{sgn}(l_2^*) b'_m P(x_2 - x_1) x'_1 + \gamma^{-1} \dot{\tilde{k}}_{21}) \frac{\tilde{k}_{21}}{|l_2^*|} \\ &\quad + 2(\text{sgn}(l_2^*) b'_m P(x_2 - x_1) x'_1 + \gamma^{-1} \dot{\tilde{k}}_2) \frac{\tilde{k}_2}{|l_2^*|} + 2(\text{sgn}(l_2^*) b'_m P(x_1 - x_m) u_1 + \gamma^{-1} \dot{\tilde{l}}_{21}) \frac{\tilde{l}_{21}}{|l_2^*|} \\ &= -e'_{21} Q e_{21}. \end{aligned} \quad (2-19)$$

From (2-19), we obtain that V_{21} has a finite limit, so $e_{21}, \tilde{k}_{21}, \tilde{k}_2, \tilde{l}_{21} \in \mathcal{L}_\infty$. Because $e_{21} \in \mathcal{L}_\infty$ and $x_1 \in \mathcal{L}_\infty$, we have $x_2 \in \mathcal{L}_\infty$. This implies $k_{21}, k_2, l_{21} \in \mathcal{L}_\infty$. We have the controller (2-15) and $k_{21}, k_2, l_{21} \in \mathcal{L}_\infty$, so that we have $u_2 \in \mathcal{L}_\infty$. Therefore, all signals in the closed-loop system are bounded. From (2-19), we can establish that \dot{V}_{21} has a bounded integral, so we have $e_{21} \in \mathcal{L}_2$. This implies $\dot{V}_{21} \rightarrow 0$ for $t \rightarrow \infty$ hence $e_{21} \rightarrow 0$ for $t \rightarrow \infty$, which concludes the proof. \square

2-2-3 Synchronization of a follower to two neighbors

In this section, we try to synchronize a follower (called agent 3) to two parents neighbors (called agent 1 and 2). We assume a directed connection from agent 1 to agent 3 and from agent 2 to agent 3, i.e. the digraph is described by $\mathcal{N} = \{1, 2, 3\}$, $\mathcal{E} = \{(1, 3), (2, 3)\}$, with this directed connection, agent 1 and agent 2 can send its input and state measurement to agent 3, but not viceversa. For simplicity, we consider an unweighted directed graph, i.e. $a_{13} = a_{23} = 1$. The network under consideration is presented in Figure 2-3.

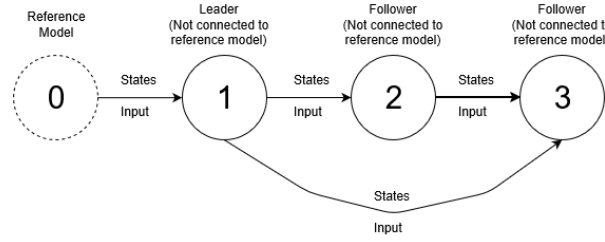


Figure 2-3: A leader-follower communication graph with two followers (state-feedback).

agent 3 is an additional follower that is connected to agent 1 and agent 2, satisfying the following dynamics:

$$\dot{x}_3 = A_3 x_3 + b_3 u_3 \quad (2-20)$$

where $x_3 \in \mathbb{R}^n$ is the state of the agent 3, $u_3 \in \mathbb{R}$ is the input. We have A_3 and b_3 are unknown matrices of appropriate dimensions. Then we propose the control law that synchronize agent 3 to agent 1 and agent 2

$$\begin{aligned} u_{31}(t) &= k'_{31}(t)x_1(t) + k'_3(t)(x_3(t) - x_1(t)) + l_{31}(t)u_1(t) \\ u_{32}(t) &= k'_{32}(t)x_2(t) + k'_3(t)(x_3(t) - x_2(t)) + l_{32}(t)u_2(t). \end{aligned} \quad (2-21)$$

In more compact form, the controller for agent 3 can be defined as the addition of $u_{31}(t)$ and $u_{32}(t)$

$$u_3(t) = k'_{31}(t)\frac{x_1(t)}{2} + k'_{32}(t)\frac{x_2(t)}{2} + k'_3(t)\frac{e_{31}(t) + e_{32}(t)}{2} + l'_{31}(t)\frac{u_1(t)}{2} + l'_{32}(t)\frac{u_2(t)}{2} \quad (2-22)$$

where $k'_{31}, k'_{32}, k'_3, l_{31}, l_{32}$ are estimates of $k^*_{31}, k^*_{32}, k^*_3, l^*_{31}, l^*_{32}$ respectively. In the interest of synchronize agent 3 to its predecessors, agent 1 and agent 2, we define the dynamics of the error $e_{31} = x_3 - x_1$ and $e_{32} = x_3 - x_2$ with dynamics

$$\begin{aligned} \dot{e}_{31} &= A_m e_{31} + b_3(u_3 - k'_{31}x_1 - k'_3 e_{31} - l^*_{31}u_1) \\ \dot{e}_{32} &= A_m e_{32} + b_3(u_3 - k'_{32}x_2 - k'_3 e_{32} - l^*_{32}u_2). \end{aligned} \quad (2-23)$$

The equation (2-23) can be derived via the dynamics of the error $e_{321} = e_{31} - e_{32}$

$$\dot{e}_{321}(t) = A_m e_{321}(t) + 2b_3(\tilde{k}'_{31}(t)\frac{x_1(t)}{2} + \tilde{k}'_{32}(t)\frac{x_2(t)}{2} + \tilde{k}'_3(t)\frac{e_{321}(t)}{2} + \tilde{l}_{31}\frac{u_1(t)}{2} + \tilde{l}_{32}\frac{u_2(t)}{2}). \quad (2-24)$$

The following Theorem provides the synchronization of a follower to two neighbors.

Theorem 3. Consider the unknown leader dynamics (2-2), the unknown follower dynamics (agent 2) (2-3), the unknown follower dynamics (agent 3) (2-20), the controller (2-22), and the adaptive laws

$$\begin{aligned} \dot{k}'_{31}(t) &= -\text{sgn}(l_3^*)\gamma b'_m P(e_{31}(t) + e_{32}(t))x_1(t)' \\ \dot{k}'_{32}(t) &= -\text{sgn}(l_3^*)\gamma b'_m P(e_{31}(t) + e_{32}(t))x_2(t)' \\ \dot{k}'_3(t) &= -\text{sgn}(l_3^*)\gamma b'_m P(e_{31}(t) + e_{32}(t))(e_{31}(t) + e_{32}(t))' \\ \dot{l}_{31}(t) &= -\text{sgn}(l_3^*)\gamma b'_m P(e_{31}(t) + e_{32}(t))u_1(t) \\ \dot{l}_{32}(t) &= -\text{sgn}(l_3^*)\gamma b'_m P(e_{31}(t) + e_{32}(t))u_2(t) \end{aligned} \quad (2-25)$$

then we guarantee synchronization of the follower dynamics (agent 3) (2-20) to the leader dynamics (2-2) and the follower dynamics (agent 2) (2-3), and the convergence $e_{321} \rightarrow 0$ for $t \rightarrow \infty$.

Proof. To analytically show the asymptotic convergence of the synchronization error between agent 3, agent 2, and the leader, we can introduce the following Lyapunov function

$$V_{321} = e'_{321} P e_{321} + \text{tr}\left(\frac{\tilde{k}'_{31}\tilde{k}_{31}}{\gamma|l_3^*|}\right) + \text{tr}\left(\frac{\tilde{k}'_{32}\tilde{k}_{32}}{\gamma|l_3^*|}\right) + \text{tr}\left(\frac{\tilde{k}'_3\tilde{k}_3}{\gamma|l_3^*|}\right) + \frac{\tilde{l}_{31}^2}{\gamma|l_3^*|} + \frac{\tilde{l}_{32}^2}{\gamma|l_3^*|}. \quad (2-26)$$

Then it is possible to verify

$$\begin{aligned} \dot{V}_{321} &= e'_{321}(P A_m + A'_m P)e_{321} + 2e'_{321} P b_3(\tilde{k}'_{31}x_1 + \tilde{k}'_{32}x_2 + \tilde{k}'_3 e_{321} + \tilde{l}_{31}u_1 + \tilde{l}_{32}u_2) \\ &\quad + 2\text{tr}\left(\frac{\tilde{k}'_{31}\gamma^{-1}\dot{\tilde{k}}_{31}}{|l_3^*|}\right) + 2\text{tr}\left(\frac{\tilde{k}'_{32}\gamma^{-1}\dot{\tilde{k}}_{32}}{|l_3^*|}\right) + 2\text{tr}\left(\frac{\tilde{k}'_3\gamma^{-1}\dot{\tilde{k}}_3}{|l_3^*|}\right) + 2\frac{\tilde{l}'_{31}\gamma^{-1}\dot{\tilde{l}}_{31}}{|l_3^*|} + 2\frac{\tilde{l}'_{32}\gamma^{-1}\dot{\tilde{l}}_{32}}{|l_3^*|} \\ &= -e'_{321} Q e_{321} + 2(\text{sgn}(l_3^*)b'_m P(e_{321})x'_1 + \gamma^{-1}\dot{\tilde{k}}'_{31})\frac{\tilde{k}_{31}}{|l_3^*|} \\ &\quad + 2(\text{sgn}(l_3^*)b'_m P(e_{321})x'_2 + \gamma^{-1}\dot{\tilde{k}}'_{32})\frac{\tilde{k}_{32}}{|l_3^*|} \\ &\quad + 2(\text{sgn}(l_3^*)b'_m P(e_{321})e'_{321} + \gamma^{-1}\dot{\tilde{k}}'_3)\frac{\tilde{k}_3}{|l_3^*|} + 2(\text{sgn}(l_3^*)b'_m P(e_{321})u_1 + \gamma^{-1}\dot{\tilde{l}}'_{31})\frac{\tilde{l}_{31}}{|l_3^*|} \\ &\quad + 2(\text{sgn}(l_3^*)b'_m P(e_{321})u_2 + \gamma^{-1}\dot{\tilde{l}}'_{32})\frac{\tilde{l}_{32}}{|l_3^*|} \\ &= -e'_{321} Q e_{321}. \end{aligned} \quad (2-27)$$

From (2-27), we obtain that V_{321} has a finite limit, so $e_{321}, \tilde{k}_{31}, \tilde{k}_{32}, \tilde{k}_3, \tilde{l}_{31}, \tilde{l}_{32} \in \mathcal{L}_\infty$. Because $e_{321} \in \mathcal{L}_\infty$, $e_{31} \in \mathcal{L}_\infty$, $e_{32} = x_3 - x_2 \in \mathcal{L}_\infty$, and $x_1, x_2 \in \mathcal{L}_\infty$, we have $x_3 \in \mathcal{L}_\infty$. This implies $k_{31}, k_{32}, k_3, l_{31}, l_{32} \in \mathcal{L}_\infty$. We have controller (2-22) and $k_{31}, k_{32}, k_3, l_{31}, l_{32} \in \mathcal{L}_\infty$, so that we have $u_3 \in \mathcal{L}_\infty$. Therefore, all signals in the closed-loop system are bounded. From (2-27), we can establish that \dot{V}_{321} has a bounded integral, so we have $e_{321} \in \mathcal{L}_2$. This implies $\dot{V}_{321} \rightarrow 0$ for $t \rightarrow \infty$ hence $e_{321} \rightarrow 0$ for $t \rightarrow \infty$, which concludes the proof. \square

2-2-4 Extension to acyclic graphs

In this subsection, we show the extension of our proposed approach to the acyclic graphs MASs synchronization. Let us first consider a set of N agents

$$\dot{x}_i = A_i x_i + b_i u_i, \quad i \in \{1, \dots, N\} \quad (2-28)$$

where agent 1 is the leader that can access the reference signal r .

Assumption 3. The communication graph is a directed acyclic graph (DAG), where the leader is the root node.

It is not difficult to extend the results of Theorems 1, 2 and 3 to acyclic communication graph. Except for the leaders, which use controller (2-6) and adaptive laws (2-8), the following controller is proposed for the other agents

$$u_j = \frac{\sum_{i=1}^N a_{ij} k'_{ji}(t) x_i(t)}{\sum_{i=1}^N a_{ij}} + \frac{\sum_{i=1}^N a_{ij} k'_j(t) (x_j(t) - x_i(t))}{\sum_{i=1}^N a_{ij}} + \frac{\sum_{i=1}^N a_{ij} l_{ji}(t) u_i(t)}{\sum_{i=1}^N a_{ij}} \quad (2-29)$$

where the terms a_{ij} indicate the entries of the adjacency matrix. One can verify that, with the appropriate adjacency matrices, the adaptive controller (2-29) reduces to the special case (2-15) and (2-22). The following result holds.

Theorem 4. Consider the unknown linear agents (2-28) with reference model (2-1), controllers (2-6), (2-29), adaptive laws (2-8) and

$$\begin{aligned} \dot{k}'_{ji}(t) &= -sgn(l_j^*) \gamma b'_m P \left[\sum_{i=1}^N a_{ij} (x_j - x_i) \right] x'_i(t) \\ \dot{k}'_j(t) &= -sgn(l_j^*) \gamma b'_m P \left[\sum_{i=1}^N a_{ij} (x_j - x_i) \right] \left[\sum_{i=1}^N a_{ij} (x_j - x_i) \right]' \\ \dot{l}'_{ji}(t) &= -sgn(l_j^*) \gamma b'_m P \left[\sum_{i=1}^N a_{ij} (x_j - x_i) \right] u'_i(t) \end{aligned} \quad (2-30)$$

where k_{ji}, k_j, l_{ji} are the estimate of $k_{ji}^*, k_j^*, l_{ji}^*$ respectively. Then, all closed-loop signals are bounded and, for any (i, j) such that $a_{ij} \neq 0$, we have $e_{ji} = x_j - x_i \rightarrow 0$ as $t \rightarrow \infty$. In addition, for every agent j we have $e_j = x_j - x_m \rightarrow 0$ as $t \rightarrow \infty$.

Proof. Let us adopt similar tools as Theorems 1,2, and 3 by considering the distributed Lyapunov function

$$V_j = \sum_{j=1}^N \left[\sum_{i=0}^N a_{ij} e_{ji} \right]' P \left[\sum_{i=0}^N a_{ij} e_{ji} \right] + \sum_{j=1}^N \sum_{i=1}^N a_{ij} \text{tr} \left[\frac{\tilde{k}'_{ji} \tilde{k}_{ji}}{\gamma |l_j^*|} \right] + \sum_{j=1}^N a_{ij} \text{tr} \left[\frac{\tilde{k}'_j \tilde{k}_j}{\gamma |l_j^*|} \right] + \sum_{j=1}^N \sum_{i=1}^N a_{ij} \frac{\tilde{l}_j^2}{\gamma |l_j^*|} \quad (2-31)$$

where the index $i = 0$ is used for the reference model, i.e. $e_{j0} = e_j = x_j - x_m$, and $a_{j0} \neq 0$ only for the root node. Then, from (2-28) and (2-29), we obtain the following error dynamics

$$\begin{aligned} \dot{e}_{ji} &= A_m e_{ji} + b_j (u_j - k_{ji}^* x_i - k_j^* e_{ji} - l_{ji}^* u_i) \\ &= A_m e_{ji} + b_j (\tilde{k}_{ji}^* x_i - \tilde{k}_j^* e_{ji} - \tilde{l}_{ji}^* u_i). \end{aligned} \quad (2-32)$$

Clearly, we have a similar structure as in the previously developed two-agent and three-agent case. Then, it is possible to verify that

$$\begin{aligned} \dot{V}_j &= - \sum_{j=1}^N \left[\sum_{i=0}^N a_{ij} e_{ji} \right]' Q \left[\sum_{i=0}^N a_{ij} e_{ji} \right] + 2 \left[\sum_{i=0}^N a_{ij} e_{ji} \right]' P b_j \left[\sum_{j=1}^N a_{ij} \tilde{k}'_{ji} x_i + \sum_{j=1}^N a_{ij} \tilde{k}_j e_{ji} \right. \\ &\quad \left. + \sum_{j=1}^N a_{ij} \tilde{l}_{ji} u_i \right] + \sum_{i=1}^N \sum_{j=1}^N a_{ij} \text{tr} \left[\frac{\tilde{k}'_{ji} \dot{\tilde{k}}_{ji}}{\gamma |l_j^*|} \right] + \sum_{j=1}^N \text{tr} \left[\frac{\tilde{k}'_j \dot{\tilde{k}}_j}{\gamma |l_j^*|} \right] + \sum_{i=1}^N \sum_{j=1}^N a_{ij} \text{tr} \left[\frac{\tilde{l}'_{ji} \dot{\tilde{l}}_{ji}}{\gamma |l_j^*|} \right] \\ &= - \sum_{j=1}^N \left[\sum_{i=0}^N a_{ij} e_{ji} \right]' Q \left[\sum_{i=0}^N a_{ij} e_{ji} \right]. \end{aligned} \quad (2-33)$$

This can be used to derive boundedness of all closed-loop signals and convergence of e_{ji} to zero, which can be proved by using the Barbalat's Lemma procedure already adopted in Theorems 1, 2, and 3. This concludes the proof. \square

2-3 Output-feedback MRAC

This section is part of [31]. The main task in this section is to find the control laws u for each agent that guarantee synchronization of MASs with unknown linear dynamics by only using the input and the output of the neighbors. In order to facilitate the main result, let us assume that there are three agents denoted with subscripts 0, 1, and 2. Let us consider the same network depicted in Figure 2-4. Here, the purpose of agent 1, the leader, is to follow agent 0. At the same time, the purpose of agent 2 is to follow agent 1. agent 0 is a reference model that is connected to agent 1, satisfying the following dynamics:

$$y_m = G_m(s) = k_m \frac{Z_m(s)}{R_m(s)} r \quad (2-34)$$

where $r \in \mathbb{R}$ and $y_m \in \mathbb{R}$ are the reference input and the output of the reference model. $Z_m(s)$ and $R_m(s)$ are known monic polynomials, and k_m is the high-frequency gain. Next, we have agents 1 and 2, denoted with subscripts 1 and 2, respectively, and with dynamics expressed in the transfer function form as

$$y_1 = G_1(s) = k_1 \frac{Z_1(s)}{R_1(s)} u_1 \quad (2-35)$$

$$y_2 = G_2(s) = k_2 \frac{Z_2(s)}{R_2(s)} u_2 \quad (2-36)$$

where $u_1, u_2 \in \mathbb{R}$, and $y_1, y_2 \in \mathbb{R}$ are the inputs and the outputs of two agents. $Z_1(s)$, $Z_2(s)$, $R_1(s)$, and $R_2(s)$ are unknown monic polynomials, and k_1 and k_2 are constants referred to the high frequency gains. Note that, possibly, $Z_1(s) \neq Z_2(s)$ and $R_1(s) \neq R_2(s)$ (heterogeneous agents with unknown dynamics). We assume a directed connection from agent 1 to agent 2, i.e., the digraph is described by $\mathcal{N} = \{1, 2\}$, $\mathcal{E} = \{(1, 2)\}$. By using this configuration, agent 2 can observe the measurement from agent 1, but not vice versa. The synchronization task between agent 0 and agent 1 is achieved when $y_1 \rightarrow y_m$

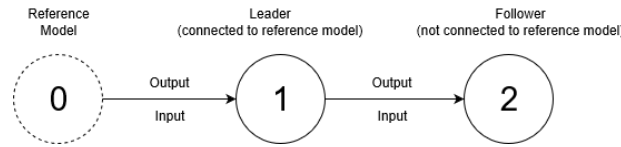


Figure 2-4: A leader-follower communication graph with one follower (output-feedback).

for $t \rightarrow \infty$. As the signal from the reference model is known to agent 1 only, the purpose of agent 2 is to follow agent 1. In this case, the synchronization task is achieved when $y_2 \rightarrow y_1$ for $t \rightarrow \infty$. It is clear that, if both synchronization tasks are achieved, then we have also $y_2 \rightarrow y_m$ for $t \rightarrow \infty$. These tasks should be achieved for any bounded reference signal r .

Assumption 4. To achieve the synchronization objectives, we need the following assumptions for the reference model (R) and the agents (A):

- (R1) $Z_m(s)$ and $R_m(s)$ are monic Hurwitz polynomials, where the degree of $R_m(s)$ is less than or equal to the relative degree of $R_i(s)$, n .
- (R2) The relative degree of $G_m(s)$ is the same as that of $G_i(s)$, $i \in \{1, 2\}$.
- (A1) $Z_i(s)$, $i \in \{1, 2\}$ are monic Hurwitz polynomials.
- (A2) An upper bound n of the degree n_i of $R_i(s)$, i.e., $i \in \{1, 2\}$, is known.
- (A3) The relative degree $n^* = n_i - m_i$ of $G_i(s)$, i.e., $i \in \{1, 2\}$, is known, where m is the degree of the numerator. The relative degree of the agents and the reference should be the same.

(A4) The sign of the high frequency gains k_i i.e., $i \in \{1, 2\}$ is known.

Remark 4. Assumption 4 is standard in output-feedback MRAC [30, Chapter 5]. Therefore, we can adopt the same assumptions also in the setting of adaptive synchronization of MASs.

In the next subsection, the synchronization of agent 1 to a reference model will be discussed.

2-3-1 Synchronization of a leader to a reference model

As classical MRAC was used for the SISO plant in Chapter 5 of [30], it is well known that the agents 1 can be synchronized to the reference model by using the following control law:

$$u_1 = l_1^{*'} \frac{\alpha(s)}{\Lambda(s)} u_1 + f_1^{*'} \frac{\alpha(s)}{\Lambda(s)} y_1 + g_1^* y_1 + c_1^* r \quad (2-37)$$

where $\Lambda(s)$ is a Hurwitz monic polynomial and α are defined as

$$\begin{aligned} \alpha(s) &= \begin{bmatrix} s^{n-2} & s^{n-3} & \dots & s & 1 \end{bmatrix} \quad \text{for } n \geq 2 \\ \alpha(s) &= 0 \quad \text{for } n = 1 \\ \Lambda(s) &= s^{n-1} + \lambda_{n-2}s^{n-2} + \dots + \lambda_1 s + \lambda_m = \Lambda_m Z_m. \end{aligned} \quad (2-38)$$

The consequence of Assumption 4 is that there are scalars $l_i^{*'}, f_i^{*'}, g_i^{*'},$ and c_i^{*}' that match the condition of agent i and the reference model such that

$$\frac{c_i^* k_i}{R_i(s)(\Lambda(s) - l_i^{*'} \alpha) - k_i Z_i(s)(f_i^{*'} \alpha + g_i^* \Lambda(s))} = \frac{k_m}{R_m(s) Z_i(s) \Lambda_m(s)}. \quad (2-39)$$

The matching conditions for agent 1 to the reference model can be defined as follows, in line with Chapter 5 in [30].

$$\begin{aligned} c_1^* k_1 &= k_m \\ R_1(s)(\Lambda(s) - l_1^{*'} \alpha) - k_1 Z_1(s)(f_1^{*'} \alpha + g_1^* \Lambda(s)) &= Z_1(s) R_m(s) \Lambda_m(s) \end{aligned} \quad (2-40)$$

where $c_1^* = \frac{k_m}{k_1}$. Being the parameters of agent 1 are unknown, the proposed control law (2-37) cannot be used for agent 1, then we can come up with

$$u_1 = l_1' \frac{\alpha}{\Lambda(s)} u_1 + f_1' \frac{\alpha}{\Lambda(s)} y_1 + g_1 y_1 + c_1 r \quad (2-41)$$

where the controller parameter vector $l_1', f_1', g_1,$ and c_1 are the estimates for $l_1^{*'}, f_1^{*'}, g_1^*,$ and $c_1^*,$ respectively. Let us assume the relative degree of 1 for simplicity. Adopting a state-space representation of the reference model and agent 1, we obtain

$$\begin{aligned} \dot{x}_m &= A_m x_m + B_m r & y_m &= h_m' x_m \\ \dot{x}_1 &= A_1 x_1 + B_1 u_1 & y_1 &= h_1' x_1. \end{aligned} \quad (2-42)$$

Let us define the state-space representation of agent 1 in the closed-loop form

$$\dot{\bar{x}}_1 = \bar{A}_1 \bar{x}_1 + \bar{B}_1 c_1^* r + \bar{B}_1 (u_1 - \theta_1^{*'} \omega_1) \quad y_1 = \bar{C}_1 \bar{x}_1 \quad (2-43)$$

where $\bar{x}_1 = [x_1' \quad \omega_{u1}' \quad \omega_{y1}']'$. \bar{A}_1 , \bar{B}_1 , and \bar{C}_1 are defined as

$$\bar{A}_1 = \begin{bmatrix} A_1 + B_1 g_1^* h_1' & B_1 l_1^{*'} & B_1 f_1^{*'} \\ dg_1^* h_1' & F + dl_1^{*'} & df_1^{*'} \\ dh_1' & 0 & F \end{bmatrix} \quad \bar{B}_1 = \begin{bmatrix} B_1 \\ d \\ 0 \end{bmatrix} \quad \bar{C}_1 = [h_1' \quad 0 \quad 0]. \quad (2-44)$$

Obviously, agent 1 can be matched to agent 0 or it can be said that $\bar{C}_1(sI - \bar{A}_1)^{-1} \bar{B}_1 c_1^* = C_m(sI - A_m)^{-1} B_m$. Therefore, the state-space representation of agent 1 in the closed-loop form could be rewritten as follows

$$\dot{\bar{x}}_1 = A_m \bar{x}_1 + B_m r + B_m \rho_1^* (u_1 - \theta_1^{*'} \omega_1) \quad y_1 = C_m \bar{x}_1 \quad (2-45)$$

where $\rho_1^* = \frac{1}{c_1^*}$. By defining the state tracking error $\tilde{x}_{10} = \bar{x}_1 - x_m$ and the output error $e_{10} = y_1 - y_m$, we obtain the error equation

$$\dot{\tilde{x}}_{10} = A_m \tilde{x}_{10} + B_m \rho_1^* \tilde{\theta}_1' \omega_1 \quad e_{10} = C_m \tilde{x}_{10} \quad (2-46)$$

where $\tilde{\theta}_1 = \theta_1 - \theta_1^*$. The following result is basically standard output-feedback MRAC.

Theorem 5. Consider the reference model dynamics (2-34), the unknown leader dynamics (2-35), the controller (2-41), and the adaptive laws

$$\begin{aligned} \dot{\omega}_{u1} &= F \omega_{u1} + d u_1 & \dot{\theta}_1 &= -\Gamma_1 e_{10} \omega_1 \operatorname{sgn}\left(\frac{k_1}{k_m}\right) \\ \dot{\omega}_{y1} &= F \omega_{y1} + d y_1 & u_1 &= \theta_1' \omega_1 \end{aligned} \quad (2-47)$$

where $e_{10} = y_1 - y_m$, $\Gamma_1 = \Gamma_1' > 0$, ω_1 , F , d , and θ_1 defined as follows

$$\omega_1 = \begin{bmatrix} \omega_{u1} \\ \omega_{y1} \\ y_1 \\ r \end{bmatrix} \quad F = \begin{bmatrix} -\lambda_{n-2} & \dots & -\lambda_m \\ \mathbb{1}_{n-2} & & 0 \end{bmatrix} \quad d = \begin{bmatrix} 1 \\ 0 \\ \vdots \\ 0 \end{bmatrix} \quad \theta_1' = [l_1' \quad f_1' \quad g_1 \quad c_1] \quad (2-48)$$

here the adaptive gain, Γ_1 , is not taken as a scalar, as it is in most literature, but as a diagonal matrix

$$\Gamma_1 = \operatorname{diag}\{\Gamma_l, \Gamma_f, \Gamma_g, \Gamma_c\} \quad (2-49)$$

where $\Gamma_l, \Gamma_f, \Gamma_g, \Gamma_c$ are the positive real numbers to be designed. Then all closed loop signals will then be bounded and the errors will converge asymptotically to zero.

Proof. To show analytically the asymptotic convergence of the synchronization error between the leader and the model reference, let us define the following Lyapunov function

$$V_1(\tilde{\theta}_1, \tilde{x}_{10}) = \frac{\tilde{x}_{10}' P \tilde{x}_{10}}{2} + \frac{\tilde{\theta}_1' \Gamma_1^{-1} \tilde{\theta}_1}{2} |\rho_1^*| \quad (2-50)$$

where $P = P' > 0$ satisfies the Kalman-Yakubovich Lemma

$$P A_m + A_m' P = -q q' - v L \quad P B_m = C_m \quad (2-51)$$

where $L = L' > 0$, and $v > 0$. One can verify the time derivative of V_1 :

$$\dot{V}_1 = -\frac{\tilde{x}_{10}' q q' \tilde{x}_{10}}{2} - \frac{v}{2} \tilde{x}_{10}' L \tilde{x}_{10} + P B_m \tilde{x}_{10} \rho_1^* \tilde{\theta}_1' \omega_1 + \tilde{\theta}_1' \Gamma_1^{-1} \dot{\tilde{\theta}}_1 |\rho_1^*|. \quad (2-52)$$

Since $P B_m \tilde{x}_{10} = C_m \tilde{x}_{10} = e_{10}$ and $\rho_1^* = |\rho_1^*| \text{sgn}(\rho_1^*)$, we can delete the indefinite term by choosing

$$\dot{\tilde{\theta}}_1 = -\Gamma_1 e_{10} \omega_1 \text{sgn}(\rho_1^*) \quad (2-53)$$

which leads to

$$\dot{V}_1 = -\frac{\tilde{x}_{10}' q q' \tilde{x}_{10}}{2} - \frac{v}{2} \tilde{x}_{10}' L \tilde{x}_{10}. \quad (2-54)$$

From (2-54), we obtain that V_1 has a finite limit, so $\tilde{x}_{10}, \tilde{\theta}_1 \in \mathcal{L}_\infty$. Because $\tilde{x}_{10} = \bar{x}_1 - \bar{x}_m \in \mathcal{L}_\infty$ and $\bar{x}_m \in \mathcal{L}_\infty$, we have $\bar{x}_1 \in \mathcal{L}_\infty$. This implies $x_1, y_1, \omega_1, \omega_2 \in \mathcal{L}_\infty$. From $u_1 = \theta_1' \omega_1$ and $\theta_1, \omega_1 \in \mathcal{L}_\infty$, we have $u_1 \in \mathcal{L}_\infty$. Therefore, all signals in the closed-loop system are bounded. From (2-54), we can establish that \dot{V}_1 has a bounded integral, so we have $\tilde{x}_{10}, e_{10} \in \mathcal{L}_2$. Furthermore, using $\theta_1, \omega_1, \tilde{x}_{10} \in \mathcal{L}_\infty$, in (2-46), we have $e_{10}, \dot{\tilde{x}}_{10} \in \mathcal{L}_\infty$. This implies $e_{10} \rightarrow 0$ for $t \rightarrow \infty$, which concludes the proof. \square

Remark 5. It is known that Theorem 5 requires the agent to obtain the reference signal r to synchronize to its neighbors which is not possible in a distributed setting. Therefore, the signals of neighboring agents will be utilized instead of the reference signal.

In relative degree 2 case ($n^* = 2$), an extra filter is introduced to synchronize the agents with the model reference. The extra-filter and the new form of the control law are defined as follows:

$$\dot{\phi}_1 = -\rho \phi_1 + \omega_1 \quad \dot{\theta}_1 = -\Gamma_1 e_{10} \phi_1 \text{sgn}\left(\frac{k_1}{k_m}\right) \quad u_1 = \theta_1' \omega_1 + \dot{\theta}_1' \phi_1 \quad (2-55)$$

where $\rho > 0$ is to be designed. Using similar Lyapunov arguments as before, one can prove $e_{10} \rightarrow 0$ for $t \rightarrow \infty$ [30]. The complexity of the methods increases with the relative degree n^* of the agent. In the next subsection, the synchronization of agent 2 to a leader node will be discussed.

2-3-2 Synchronization of a follower to a neighbor

The control law (2-37) and consequently the matching condition (2-39) have two problems. The first problem is that the transfer function G_1 of the agents is unknown, and we do not know the $l_1^{*'}, f_1^{*'}, g_1^*$, and c_1^* . The second problem is that, even if the transfer function were known, the control law (2-37) would be implementable only for those agents connected to the reference model, agent 0, and with access to r . Therefore, we cannot implement the control law (2-37) for agent 2. In place of the matching condition between agent 2 and agent 0, we should formulate a matching condition between agent 2 and agent 1. The following proposition follows.

Proposition 2. There is an ideal control law that matches an agent to its neighbor in the form

$$u_2 = l_{21}^{*'} \frac{\alpha}{\Lambda(s)} u_1 + f_{21}^{*'} \frac{\alpha}{\Lambda(s)} y_1 + g_{21}^* y_1 + c_{21}^* u_1 + l_2^{*'} \frac{\alpha}{\Lambda(s)} (u_2 - u_1) + f_2^{*'} \frac{\alpha}{\Lambda(s)} (y_2 - y_1) + g_2^* (y_2 - y_1) \quad (2-56)$$

where the gains satisfy the following matching conditions

$$R_1(s)(\Lambda(s) - (\bar{l}_2^{*'} - \bar{l}_{21}^{*'})\alpha) - Z_1(s)k_2((f_2^{*'} - f_{21}^{*'})\alpha + \Lambda(s)(g_2^* - g_{21}^*)) = Z_1(s)\Lambda_m(s)R_m(s) \quad (2-57)$$

Proof. In this proof, we want to formulate the matching conditions for agent 2 to agent 1 by using the proposed control law for agent 2. First, let us rewrite the control law (2-56) as follows:

$$(1 - l_2^{*'} \frac{\alpha}{\Lambda(s)})u_2 = (l_{21}^{*'} - l_2^{*'}) \frac{\alpha}{\Lambda(s)} u_1 + (f_{21}^{*'} - f_2^{*'}) \frac{\alpha}{\Lambda(s)} y_1 + (g_{21}^* - g_2^*)y_1 + l_2^{*'} \frac{\alpha}{\Lambda(s)} y_2 + g_2^* y_2 + c_{21}^* u_1$$

$$u_2 = \frac{(l_{21}^{*'} - l_2^{*'}) \alpha u_1 + (f_{21}^{*'} - f_2^{*'}) \alpha y_1 + \Lambda(s)(g_{21}^* - g_2^*)y_1 + l_2^{*'} \alpha y_2 + g_2^* y_2 \Lambda(s) + c_{21}^* u_1 \Lambda(s)}{(\Lambda(s) - l_2^{*'} \alpha)} \quad (2-58)$$

Substitute the control law in (2-58) to (2-35) and use the following matching condition of agent 2 to reference model

$$R_2(s)(\Lambda(s) - l_2^{*'} \alpha) - k_2 Z_2(s)(f_2^{*'} \alpha + \Lambda(s)g_2^*) = Z_2(s)R_m(s)\Lambda_m(s) \quad (2-59)$$

which leads to

$$(Z_2(s)\Lambda_m(s)R_m(s))(y_2 - y_1) + (R_2(s)(\Lambda(s) - l_2^{*'} \alpha) - k_2 Z_2(s)(f_2^{*'} \alpha + \Lambda(s)g_2^*))y_1 =$$

$$k_2 Z_2(s)c_{21}^* (\Lambda(s) + \frac{l_{21}^{*'}}{c_{21}^*} \alpha - \frac{l_2^{*'}}{c_{21}^*} \alpha)u_1. \quad (2-60)$$

Then (2-60) can be written as follows:

$$R_1(s)(\Lambda(s) - (\bar{l}_2^{*'} - \bar{l}_{21}^{*'})\alpha) - Z_1(s)k_2((f_2^{*'} - f_{21}^{*'})\alpha + \Lambda(s)(g_2^* - g_{21}^*)) = Z_1(s)\Lambda_m(s)R_m(s) \quad (2-61)$$

where $c_{21}^* = \frac{k_1}{k_2}$, $\bar{l}_{21}^* = \frac{l_{21}^*}{c_{21}^*}$, and $\bar{l}_2^* = \frac{l_2^*}{c_{21}^*}$. This concludes the proof. \square

Remark 6. Proposition 2 shows us a distributed matching condition among neighboring agents in synchronization of MASs (output-feedback case). In other words, there exist gains that match an agent to its neighbors. Such distributed matching condition has been derived without extra assumptions than the standard assumptions of adaptive control.

Being the parameters of agent 2 are unknown, the proposed control (2-56) cannot be used for agent 2, then we can come up with

$$u_2 = l'_{21} \frac{\alpha}{\Lambda(s)} u_1 + f'_{21} \frac{\alpha}{\Lambda(s)} y_1 + g_{21} y_1 + c_{21} u_1 + l'_2 \frac{\alpha}{\Lambda(s)} (u_2 - u_1) + f'_2 \frac{\alpha}{\Lambda(s)} (y_2 - y_1) + g_2 (y_2 - y_1) \quad (2-62)$$

where the controller parameter vector l'_{21} , l'_2 , f'_{21} , f'_2 , g_{21} , g_1 , and c_{21} are the estimates for l_{21}^* , l_2^* , f_{21}^* , f_2^* , g_{21}^* , g_1^* , and c_{21}^* , respectively. First let us consider agent 2 with dynamics

$$\dot{x}_2 = A_2 x_2 + B_2 u_2 \quad y_2 = h'_2 x_2. \quad (2-63)$$

The closed-loop form allows us to write

$$\dot{\bar{x}}_2 = \bar{A}_2 \bar{x}_2 + \bar{B}_2 c_{21}^* \bar{u}_2 + \bar{B}_2 (u_2 - \theta_2^{*'} \omega_2) \quad y_2 = \bar{C}_2 \bar{x}_2 \quad (2-64)$$

where $\bar{x}_2 = [x'_2 \quad \omega'_{u_1} \quad \omega'_{y_1} \quad \omega'_{u_{21}} \quad \omega'_{y_{21}}]'$ and $\bar{u}_2 = [u_1 \quad y_1]'$.

$$\bar{A}_2 = \begin{bmatrix} A_2 + B_2 g_2^* h'_2 & B_2 l_{21}^{*'} & B_2 f_{21}^{*'} & B_2 l_2^{*'} & B_2 f_2^{*'} \\ 0 & F & 0 & 0 & 0 \\ dh'_2 & 0 & F & 0 & 0 \\ dg_2^* h'_2 & dl_{21}^* & df_{21}^* & F + dl_2^* & df_2^* \\ dh'_2 & 0 & 0 & 0 & F \end{bmatrix}, \quad \bar{B}_2 = \begin{bmatrix} B_2 & \frac{B_2(g_{21}^* - g_2^*)}{c_{21}^*} \\ \frac{d}{c_{21}^*} & 0 \\ 0 & \frac{d}{c_{21}^*} \\ d(1 - \frac{1}{c_{21}^*}) & \frac{d(g_{21}^* - g_2^*)}{c_{21}^*} \\ 0 & -\frac{d}{c_{21}^*} \end{bmatrix}$$

$$\bar{C}_2 = [h'_2 \quad 0 \quad 0 \quad 0 \quad 0]. \quad (2-65)$$

From Equation (2-61), we already know that agent 2 can match agent 1 or it can be defined as $\bar{C}_2(sI - \bar{A}_2)^{-1} \bar{B}_2 c_{21}^* = \bar{C}_1(sI - \bar{A}_1)^{-1} \bar{B}_1 c_1^*$. Therefore, agent 2 can match the reference model $\bar{C}_2(sI - \bar{A}_2)^{-1} \bar{B}_2 c_{21}^* = C_m(sI - A_m)^{-1} B_m$. We can then take a non-nominal state-space representation of agent 2:

$$\dot{\bar{x}}_2 = A_m \bar{x}_2 + B_m r + B_m \rho_2^* (u_2 - \theta_2^{*'} \omega_2) \quad y_2 = C_m \bar{x}_2 \quad (2-66)$$

where $\rho_2^* = \frac{1}{c_{21}^*}$. By defining the state tracking error $\tilde{x}_{21} = \bar{x}_2 - \bar{x}_1$, and the output error $e_{21} = y_2 - y_1$, let us define the following error dynamics:

$$\begin{aligned} \dot{\tilde{x}}_{21} &= A_m \tilde{x}_{21} + B_m \rho_2^* (u_2 - \theta_2^{*'} \omega_2) \\ &= A_m \tilde{x}_{21} + B_m \rho_2^* \tilde{\theta}_2^{*'} \omega_2 \\ e_{21} &= C_m \tilde{x}_{21} \end{aligned} \quad (2-67)$$

where $\tilde{\theta}_2^* = \theta_2 - \theta_2^*$. The following Theorem provides the leader-follower synchronization.

Theorem 6. Consider the unknown leader dynamics (2-35), the unknown follower dynamics (2-36), controllers (2-62), and the adaptive laws

$$\begin{aligned} \dot{\omega}_{u_1} &= F\omega_{u_1} + du_1 & \dot{\omega}_{u_{21}} &= F\omega_{u_{21}} + d(u_2 - u_1) & \dot{\theta}_2 &= -\Gamma_2 e_{21} \omega_2 \operatorname{sgn}\left(\frac{k_2}{k_m}\right) \\ \dot{\omega}_{y_1} &= F\omega_{y_1} + dy_1 & \dot{\omega}_{y_{21}} &= F\omega_{y_{21}} + d(y_2 - y_1) & u_2 &= \theta_2' \omega_2 \end{aligned} \quad (2-68)$$

where $e_{21} = y_2 - y_1$.

$$\begin{aligned} \omega_2 &= \begin{bmatrix} \omega_{u_1}' \\ \omega_{y_1}' \\ y_1 \\ u_1 \\ \omega_{u_{21}}' \\ \omega_{y_{21}}' \\ y_2 - y_1 \end{bmatrix} & F &= \begin{bmatrix} -\lambda_{n-2} & \dots & -\lambda_m \\ \mathbf{1}_{n-2} & & 0 \end{bmatrix} & d &= \begin{bmatrix} 1 \\ 0 \\ \vdots \\ 0 \end{bmatrix} & \theta_2' &= [l_{21}' \quad f_{21}' \quad g_{21} \quad c_{21} \quad l_2' \quad f_2' \quad g_2] \\ \Lambda(s) &= s^{n-1} + \lambda_{n-2}s^{n-2} + \dots + \lambda_1 s + \lambda_m & \Gamma_2 &= \operatorname{diag}\{\Gamma_l, \Gamma_f, \Gamma_g, \Gamma_c, \Gamma_l, \Gamma_f, \Gamma_g\} \end{aligned} \quad (2-69)$$

where $\Gamma_l, \Gamma_f, \Gamma_g, \Gamma_c$ are the positive real numbers to be designed. Then all closed-loop signals are bounded and the errors converge asymptotically to zero.

Proof. To show analytically the asymptotic converge of the synchronization error, the Lyapunov-based approach will be used.

$$V_2(\tilde{\theta}_2, \tilde{x}_{21}) = \frac{\tilde{x}_{21}' P \tilde{x}_{21}}{2} + \frac{\tilde{\theta}_2' \Gamma_2^{-1} \tilde{\theta}_2}{2} |\rho_2^*| \quad (2-70)$$

where $\Gamma_2 = \Gamma_2' > 0$ and $P = P' > 0$ such that (2-51) holds. The time derivative (2-70) along the trajectory of (2-67) is given by

$$\dot{V}_2 = -\frac{\tilde{x}_{21}' q q' \tilde{x}_{21}}{2} - \frac{v}{2} \tilde{x}_{21}' L \tilde{x}_{21} + P B_m \tilde{x}_{21} \rho_2^* \tilde{\theta}_2' \omega_2 + \tilde{\theta}_2' \Gamma_2^{-1} \dot{\tilde{\theta}}_2 |\rho_2^*|. \quad (2-71)$$

Since $P B_m \tilde{x}_{21} = \bar{C}_m \tilde{x}_{21} = e_{21}$ and $\rho_2^* = |\rho_2^*| \operatorname{sgn}(\rho_2^*)$, we can delete the indefinite term by choosing

$$\dot{\tilde{\theta}}_2 = -\Gamma_2 e_{21} \omega_2 \operatorname{sgn}(\rho_2^*) \quad (2-72)$$

which leads to

$$\dot{V}_2 = -\frac{\tilde{x}_{21}' q q' \tilde{x}_{21}}{2} - \frac{v}{2} \tilde{x}_{21}' L \tilde{x}_{21}. \quad (2-73)$$

From (2-73), we obtain that V_2 has a finite limit, so $\tilde{x}_{21}, \tilde{\theta}_2 \in \mathcal{L}_\infty$. Because $\tilde{x}_{21} = \bar{x}_2 - \bar{x}_1 \in \mathcal{L}_\infty$ and $\bar{x}_1 \in \mathcal{L}_\infty$, we have $\bar{x}_2 \in \mathcal{L}_\infty$. This implies $x_2, y_2, \omega_{u_1}, \omega_{y_1}, \omega_{u_{21}}, \omega_{y_{21}} \in \mathcal{L}_\infty$. From $u_2 = \theta_2' \omega_2$ and $\theta_2, \omega_2 \in \mathcal{L}_\infty$, we have $u_2 \in \mathcal{L}_\infty$. Therefore, all signals in the closed-loop system are bounded. From (2-73) we can establish that \dot{V}_2 has a bounded integral, so we have $\tilde{x}_{21}, e_{21} \in \mathcal{L}_2$. Furthermore, using $\theta_2, \omega_2, \tilde{x}_{21} \in \mathcal{L}_\infty$ in (2-67), we have $e_{21}, \tilde{\dot{x}}_{21} \in \mathcal{L}_\infty$. This concludes the proof of the boundedness of all closed-loop signals and convergence $e_{21} \rightarrow 0$ for $t \rightarrow \infty$. \square

2-3-3 Synchronization of a follower to two neighbors

Before giving the main result, it is necessary to deal with the case in which a follower (called agent 3) tries to synchronize two parent neighbors (called agents 1 and 2). Let us assume a directed connection from 1 to 3 and from 2 to 3. The digraph is described by $\mathcal{N} = \{1, 2, 3\}$, $\mathcal{E} = \{(1, 3), (2, 3)\}$. In addition, let us consider for simplicity an unweighted digraph, i.e., $a_{12} = a_{13} = a_{23} = 1$, and the edges' weights are equal to 1. The network under the consideration is presented in Figure 2-5. We have agent 3

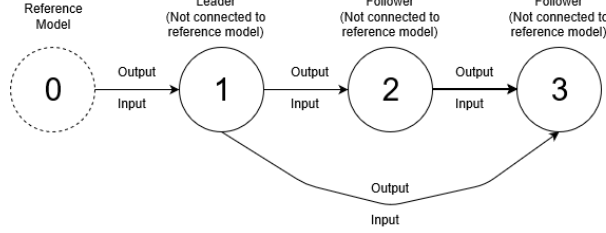


Figure 2-5: A leader-follower directed communication graph with two followers (output-feedback).

denoted with subscript 3 and dynamics expressed in the transfer function form:

$$y_3 = G_3(s) = k_3 \frac{Z_3(s)}{R_3(s)} u_3 \quad (2-74)$$

where $u_3 \in \mathbb{R}$ and $y_3 \in \mathbb{R}$ are the input and the output of agent 3. $Z_3(s)$ and $R_3(s)$ are unknown monic polynomials, and k_3 is a constant referred to the high frequency gains. Note that, possibly, $Z_3(s) \neq Z_1(s)$, $Z_3(s) \neq Z_2(s)$, and $R_3(s) \neq R_1(s)$, $R_3(s) \neq R_2(s)$ (heterogeneous agents with unknown dynamics). We assume a directed connection from agent 1 to agent 3 and a directed connection from agent 2 to agent 3. By using this configuration, agent 3 can observe measurement from agent 1 and agent 2, respectively, but not vice versa. By following an approach similar to that taken in the previous subsection (cf. Proposition 2), the synchronization of agent 3 to agent 1 is possible via the controller.

$$\begin{aligned} u_3 &= l'_{31} \frac{\alpha}{\Lambda(s)} u_1 + f'_{31} \frac{\alpha}{\Lambda(s)} y_1 + g_{31} y_1 + c_{31} u_1 + l'_3 \frac{\alpha}{\Lambda(s)} u_{31} + f'_3 \frac{\alpha}{\Lambda(s)} e_{31} + g_3 e_{31} \\ &= \theta'_{31} \omega_{31} \end{aligned} \quad (2-75)$$

and the synchronization of agent 3 to agent 2 is possible via the controller

$$\begin{aligned} u_3 &= l'_{32} \frac{\alpha}{\Lambda(s)} u_2 + f'_{32} \frac{\alpha}{\Lambda(s)} y_2 + g_{32} y_2 + c_{32} u_2 + l'_3 \frac{\alpha}{\Lambda(s)} u_{32} + f'_3 \frac{\alpha}{\Lambda(s)} e_{32} + g_3 e_{32} \\ &= \theta'_{32} \omega_{32} \end{aligned} \quad (2-76)$$

where $u_{31} = u_3 - u_1$ and $u_{32} = u_3 - u_2$, and the output error $e_{31} = y_3 - y_1$, $e_{32} = y_3 - y_2$. In a more compact form, the controller for agent 3 can be defined as the addition of

(2-75) and (2-76):

$$\begin{aligned}
 u_3 &= l'_{31} \frac{\alpha}{2\Lambda(s)} u_1 + f'_{31} \frac{\alpha}{2\Lambda(s)} y_1 + \frac{g_{31} y_1}{2} + \frac{c_{31} u_1}{2} + l'_{32} \frac{\alpha}{2\Lambda(s)} u_2 + f'_{32} \frac{\alpha}{2\Lambda(s)} y_2 + \frac{g_{32} y_2}{2} \\
 &+ \frac{c_{32} u_2}{2} + l'_3 \frac{\alpha}{2\Lambda(s)} u_{321} + f'_3 \frac{\alpha}{2\Lambda(s)} e_{321} + \frac{g_3 e_{321}}{2} \\
 &= \frac{\theta'_3 \omega_3}{2}
 \end{aligned} \tag{2-77}$$

where $u_{321} = u_{31} + u_{32}$, $e_{321} = e_{31} + e_{32}$, $\theta_3 = \theta_{31} + \theta_{32}$, and $\omega_3 = \omega_{31} + \omega_{32}$. The following Theorem provides the synchronization of a follower to two neighbors.

Theorem 7. Consider the unknown leader dynamics (2-35), the unknown follower dynamics (agent 2) (2-36), the unknown follower dynamics (agent 3) (2-74), the controllers (2-77), and the adaptive laws

$$\begin{aligned}
 \dot{\omega}_{u_1} &= F\omega_{u_1} + du_1 & \dot{\omega}_{y_1} &= F\omega_{y_1} + dy_1 \\
 \dot{\omega}_{u_2} &= F\omega_{u_2} + du_2 & \dot{\omega}_{y_2} &= F\omega_{y_2} + dy_2 \\
 \dot{\omega}_{u_{321}} &= F\omega_{u_{321}} + du_{321} & \dot{\omega}_{e_{321}} &= F\omega_{e_{321}} + de_{321} \\
 \dot{\theta}_3 &= -\Gamma_3 e_{321} \omega_3 \text{sgn}\left(\frac{k_3}{k_m}\right) & u_3 &= \frac{\theta'_3 \omega_3}{2}
 \end{aligned} \tag{2-78}$$

where

$$\begin{aligned}
 \omega'_3 &= [\omega_{u_1} \ \omega_{y_1} \ y_1 \ u_1 \ \omega_{u_2} \ \omega_{y_2} \ y_2 \ u_2 \ \omega_{u_{321}} \ \omega_{e_{321}} \ e_{321}] \\
 \theta'_3 &= [l'_{31} \ f'_{31} \ g_{31} \ c_{31} \ l'_{32} \ f'_{32} \ g_{32} \ c_{32} \ l'_3 \ f'_3 \ g_3] \\
 F &= \begin{bmatrix} -\lambda_{n-2} & \cdots & -\lambda_m \\ I_{n-2} & & 0 \end{bmatrix} \quad d' = \begin{bmatrix} 1 & 0 & \cdots & 0 \end{bmatrix} \\
 \Lambda(s) &= s^{n-1} + \lambda_{n-2}s^{n-2} + \cdots + \lambda_1 s + \lambda_m \\
 \Gamma_3 &= \text{diag}\{\Gamma_l, \Gamma_f, \Gamma_g, \Gamma_c, \Gamma_l, \Gamma_f, \Gamma_g, \Gamma_c, \Gamma_l, \Gamma_f, \Gamma_g\}.
 \end{aligned} \tag{2-79}$$

Then, all closed-loop signals are bounded and the errors converge asymptotically to zero.

Proof. To show analytically the asymptotic convergence of the synchronization error, the Lyapunov-based approach will be used. Let us define the dynamics error $\tilde{x}_{31} = \bar{x}_3 - \bar{x}_1$, $\tilde{x}_{32} = \bar{x}_3 - \bar{x}_2$, and $\tilde{x}_{321} = \bar{x}_{31} + \bar{x}_{32}$. Following the same approach in the previous section, let us derive the dynamics error e_{321} :

$$\begin{aligned}
 \dot{\tilde{x}}_{321} &= A_m \tilde{x}_{321} + B_m \rho_{31}^* (u_3 - \theta_{31}^* \omega_{31}) + B_m \rho_{32}^* (u_3 - \theta_{32}^* \omega_{32}) \\
 &= A_m \tilde{x}_{321} + 2B_m \rho_{321}^* \tilde{\theta}_3^* \omega_3^* \\
 e_{321} &= C_m \tilde{x}_{321}
 \end{aligned} \tag{2-80}$$

where $\tilde{\theta}_{31}^* = \theta_{31} - \theta_{31}^*$, $\tilde{\theta}_{32}^* = \theta_{32} - \theta_{32}^*$, $\tilde{\theta}_3^* = \tilde{\theta}_{31}^* + \tilde{\theta}_{32}^*$, and $\rho_{321}^* = \rho_{31}^* + \rho_{32}^*$. One can take the Lyapunov function:

$$V_3(\tilde{\theta}_3, \tilde{x}_{321}) = \frac{\tilde{x}_{321}' P \tilde{x}_{321}}{2} + \frac{\tilde{\theta}_3' \Gamma_3^{-1} \tilde{\theta}_3}{2} |\rho_{321}^*| \quad (2-81)$$

where $\Gamma_3 = \Gamma_3' > 0$ and $P = P' > 0$ such that (2-51) holds. The time derivative (2-81) along (2-80) is given by

$$\dot{V}_3 = -\frac{\tilde{x}_{321}' q q' \tilde{x}_{321}}{2} - \frac{v}{2} \tilde{x}_{321}' L \tilde{x}_{321} + P B_m \tilde{x}_{321} \rho_{321}^* \tilde{\theta}_3' \omega_3 + \tilde{\theta}_3' \Gamma_3^{-1} \dot{\tilde{\theta}}_3 |\rho_{321}^*|. \quad (2-82)$$

Since $P B_m \tilde{x}_{321} = C_m \tilde{x}_{321} = e_{321}$ and $\rho_{321}^* = |\rho_{321}^*| \text{sgn}(\rho_{321}^*)$, we can delete the indefinite term by choosing

$$\dot{\tilde{\theta}}_3 = \dot{\theta}_3 = -\Gamma_3 e_{321} \omega_3 \text{sgn}(\rho_{321}^*) \quad (2-83)$$

which leads to

$$\dot{V}_3 = -\frac{\tilde{x}_{321}' q q' \tilde{x}_{321}}{2} - \frac{v}{2} \tilde{x}_{321}' L \tilde{x}_{321}. \quad (2-84)$$

From (2-84), we obtain that V_3 has a finite limit, so $\tilde{x}_{321}, \tilde{\theta}_3 \in \mathcal{L}_\infty$. Because $\tilde{x}_{321} = \bar{x}_{31} + \bar{x}_{32}$, $\tilde{x}_{31} = \bar{x}_3 - \bar{x}_1 \in \mathcal{L}_\infty$, $\tilde{x}_{32} = \bar{x}_3 - \bar{x}_2 \in \mathcal{L}_\infty$, $\bar{x}_1 \in \mathcal{L}_\infty$, and $\bar{x}_2 \in \mathcal{L}_\infty$, we have $\bar{x}_3 \in \mathcal{L}_\infty$. This implies $x_3, y_3, \omega_{u1}, \omega_{u2}, \omega_{y1}, \omega_{y2}, \omega_{u321}, \omega_{e321} \in \mathcal{L}_\infty$. From $u_3 = \tilde{\theta}_3' \omega_3$ and $\theta_3, \omega_3 \in \mathcal{L}_\infty$, we have $u_3 \in \mathcal{L}_\infty$. Therefore, all signals in the closed-loop system are bounded. From (2-84), we can establish that \dot{V}_3 has bounded integral, so we have $\tilde{x}_{321}, e_{321} \in \mathcal{L}_2$. Furthermore, using $\theta_3, \omega_3, \tilde{x}_{321} \in \mathcal{L}_\infty$ in (2-80), we have $e_{321}, \dot{\tilde{x}}_{321} \in \mathcal{L}_\infty$. This concludes the proof of the boundedness of all closed-loop signals and convergence $e_{321} \rightarrow 0$ for $t \rightarrow \infty$. \square

2-3-4 Extension to acyclic graphs

In this subsection, we show the extension of our proposed approach to the acyclic graphs MASs synchronization. Let us first consider a set of N agents

$$y_i = G_i(s) = k_i \frac{Z_i(s)}{R_i(s)} u_i, \quad i \in \{1, \dots, N\} \quad (2-85)$$

where agent 1 is the leader that can access the reference signal r . It is not difficult to extend the results of Theorems 5, 6 and 7 to acyclic communication graph. Except for the leaders, which use controller (2-41) and adaptive laws (2-47), the following controller is proposed for the other agents

$$\begin{aligned} u_j = & \frac{\sum_{i=1}^N a_{ij} l_{ji}' \omega_{ui}'}{\sum_{i=1}^N a_{ij}} + \frac{\sum_{i=1}^N a_{ij} f_{ji}' \omega_{yi}'}{\sum_{i=1}^N a_{ij}} + \frac{\sum_{i=1}^N a_{ij} g_{ji} y_i}{\sum_{i=1}^N a_{ij}} + \frac{\sum_{i=1}^N a_{ij} c_{ji} u_i}{\sum_{i=1}^N a_{ij}} \\ & + \frac{\sum_{i=1}^N a_{ij} l_{ji}' \omega_{uji}'}{\sum_{i=1}^N a_{ij}} + \frac{\sum_{i=1}^N a_{ij} f_{ji}' \omega_{yji}'}{\sum_{i=1}^N a_{ij}} + \frac{\sum_{i=1}^N a_{ij} g_{ji}' e_{ji}}{\sum_{i=1}^N a_{ij}} \end{aligned} \quad (2-86)$$

where the terms a_{ij} indicate the entries of the adjacency matrix. One can verify that, with the appropriate adjacency matrices, the adaptive controller (2-86) reduces to the special case (2-62) and (2-77). The following result holds.

Theorem 8. Consider the unknown linear agents (2-85) with reference model (2-34), controllers (2-41), (2-86), adaptive laws (2-47) and

$$\begin{aligned} \dot{\omega}_{u_i} &= F\omega_{u_i} + du_i & \dot{\omega}_{u_{ji}} &= F\omega_{u_{ji}} + d(u_j - u_i) & \dot{\theta}_j &= -\Gamma_j e_{ji} \omega_j \operatorname{sgn}\left(\frac{k_j}{k_i}\right) \\ \dot{\omega}_{y_i} &= F\omega_{y_i} + dy_i & \dot{\omega}_{y_{ji}} &= F\omega_{y_{ji}} + d(y_j - y_i) & u_j &= \theta'_j \omega_j \end{aligned} \quad (2-87)$$

where $l_{ji}, f_{ji}, g_{ji}, c_{ji}, l_j, f_j, g_j$ are the estimate of $l_{ji}^*, f_{ji}^*, g_{ji}^*, c_{ji}^*, l_j^*, f_j^*, g_j^*$ respectively. Then, all closed-loop signals are bounded and, for any (i, j) such that $a_{ij} \neq 0$, we have $e_{ji} = y_j - y_i \rightarrow 0$ as $t \rightarrow \infty$. In addition, for every agent j we have $e_j = y_j - y_m \rightarrow 0$ as $t \rightarrow \infty$.

Proof. Let us adopt similar tools as Theorems 5, 6, and 7 by considering the distributed Lyapunov function

$$V_j = \sum_{j=1}^N \left[\sum_{i=0}^N a_{ij} \tilde{x}_{ji} \right]' \frac{P}{2} \left[\sum_{i=0}^N a_{ij} \tilde{x}_{ji} \right] + \sum_{j=1}^N a_{ij} \left[\frac{\tilde{\theta}_j' \Gamma_j^{-1} \tilde{\theta}_j}{2} \right] \quad (2-88)$$

where the index $i = 0$ is used for the reference model, i.e. $\tilde{x}_{j0} = \tilde{x}_j = x_j - x_m$, and $a_{j0} \neq 0$ only for the root node. Then, from (2-85) and (2-86), we obtain the following error dynamics

$$\begin{aligned} \dot{\tilde{x}}_{ji} &= A_m \tilde{x}_{ji} + B_m \rho_j^* (u_j - \theta_j' \omega_j) \\ &= A_m \tilde{x}_{ji} + B_m \rho_j^* \tilde{\theta}_j' \omega_j \\ e_{ji} &= C_m \tilde{x}_{ji}. \end{aligned} \quad (2-89)$$

Clearly, we have a similar structure as in the previously developed two-agent and three-agent case. Then, it is possible to verify that

$$\begin{aligned} \dot{V}_j &= - \sum_{j=1}^N \left[\sum_{i=0}^N a_{ij} \tilde{x}_{ji} \right]' q q' \left[\sum_{i=0}^N a_{ij} \tilde{x}_{ji} \right] - \sum_{j=0}^N \sum_{i=1}^N a_{ij} \left[v \tilde{x}_{ji}' L \tilde{x}_{ji} \right] + \sum_{j=1}^N \left[\tilde{\theta}_j' \Gamma_j^{-1} \dot{\tilde{\theta}}_j |\rho_j| \right] \\ &\quad + \sum_{j=0}^N \sum_{i=1}^N a_{ij} \left[P B_m \tilde{x}_{ji} \rho_j^* \tilde{\theta}_j' \omega_j \right] \\ &= - \sum_{j=1}^N \left[\sum_{i=0}^N a_{ij} \tilde{x}_{ji} \right]' q q' \left[\sum_{i=0}^N a_{ij} \tilde{x}_{ji} \right] - \sum_{j=0}^N \sum_{i=1}^N a_{ij} \left[v \tilde{x}_{ji}' L \tilde{x}_{ji} \right]. \end{aligned} \quad (2-90)$$

This can be used to derive boundedness of all closed-loop signals and convergence of e_{ji} to zero, which can be proved by using the Barbalat's Lemma procedure already adopted in Theorems 5, 6, and 7. This concludes the proof. \square

2-3-5 Summary

The distributed adaptive controls based on state-feedback MRAC and output-feedback MRAC have been derived in this chapter under the matching condition assumptions. The asymptotic convergence of the synchronization error has been analytically proven by introducing an appropriately defined distributed Lyapunov function. It is known that the proposed control laws and adaptive laws work under DAG condition and fixed communication topology. The next chapter provides the approach that relaxed those conditions.

Chapter 3

Adaptive synchronization with cyclic communication network

This chapter is organized as follows: Section 3-1 provides the parameter projection assumptions to be used under a graph with cycle or undirected graph.

3-1 Well-posedness of the input

The proposed distributed adaptive control based on MRAC assumes the communication graph is DAG. In this section, we will discuss the well-posedness of the agents' input by introducing the parameter projection that will be applied on state-feedback MRAC case only. In output-feedback, such a well-posedness is unknown due to the presence of the filter. So that we only consider the state-feedback case. In order to support the main result, let us rewrite the dynamics of the reference model

$$\dot{x}_m = A_m x_m + b_m r \quad (3-1)$$

where $x_m \in \mathbb{R}^n$ is the state of the reference model, $r \in \mathbb{R}$ is its reference input, and A_m and b_m are *known* matrices of appropriate dimensions, with A_m being Hurwitz so as to have bounded state trajectories x_m . Then, we have three agents that have the dynamics

$$\begin{aligned} \dot{x}_1 &= A_1 x_1 + b_1 u_1 \\ \dot{x}_2 &= A_2 x_2 + b_2 u_2 \\ \dot{x}_3 &= A_3 x_3 + b_3 u_3 \end{aligned} \quad (3-2)$$

where $x_1, x_2, x_3 \in \mathbb{R}^n$ is the state, $u_1, u_2, u_3 \in \mathbb{R}$ is the input, and A_1, A_2, A_3 and b_1, b_2, b_3 are *unknown* matrices of appropriate dimensions, with possibly $A_1 \neq A_2 \neq A_3$

and $b_1 \neq b_2 \neq b_3$. Then we have introduced the communication graph with a cycle as in Figure 3-1.

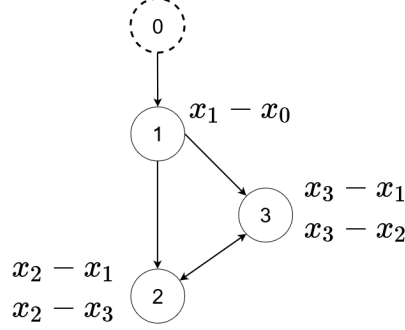


Figure 3-1: A communication graph with a cycle

The inputs to the three vehicles can be written as

$$\begin{aligned}
 u_1(t) &= k'_1(t)x_1(t) + l_1(t)r(t) \\
 2u_2(t) &= k'_{21}(t)x_1(t) + k'_2(t)(x_2(t) - x_1(t)) + l_{21}(t)u_1(t) \\
 &\quad + k'_{31}(t)x_3(t) + k'_2(t)(x_2(t) - x_3(t)) + l_{23}(t)u_3(t) \\
 2u_3(t) &= k'_{31}(t)x_1(t) + k'_3(t)(x_3(t) - x_1(t)) + l_{31}(t)u_1(t) \\
 &\quad + k'_{32}(t)x_2(t) + k'_3(t)(x_3(t) - x_2(t)) + l_{32}(t)u_2(t).
 \end{aligned} \tag{3-3}$$

or, in a more compact matrix form

$$\underbrace{\begin{bmatrix} 1 & 0 & 0 \\ -l_{21} & 2 & -l_{23} \\ -l_{31} & -l_{32} & 2 \end{bmatrix}}_U \begin{bmatrix} u_1 \\ u_2 \\ u_3 \end{bmatrix} = \begin{bmatrix} k_1 & 0 & 0 \\ k_{21} - k_2 & 2k_2 & k_{31} - k_2 \\ k_{31} - k_3 & k_{32} - k_3 & 2k_3 \end{bmatrix} \begin{bmatrix} x_1 \\ x_2 \\ x_3 \end{bmatrix} + \begin{bmatrix} l_1 \\ 0 \\ 0 \end{bmatrix} r. \tag{3-4}$$

In order to be able to say that u_1 , u_2 , and u_3 are well-posed at all time steps, we need to guarantee that the matrix U is invertible. To this purpose, let us calculate the determinant of U , so as to obtain

$$\det \begin{bmatrix} 1 & 0 & 0 \\ -l_{21} & 2 & -l_{23} \\ -l_{31} & -l_{32} & 2 \end{bmatrix} = 4 - l_{23}l_{32}. \tag{3-5}$$

In the ideal case (with the actual parameters from Proposition 1) $l_{23}^*l_{32}^* = 1$, so that the determinant of the ideal U^* is equal to 3. However, in the actual case with the estimated parameters, the determinant of U can take arbitrary values and even result equal to 0. This would make the inputs u_1 , u_2 , and u_3 not well-posed at all time steps. A simple approach to guarantee well-posedness of the inputs at all time steps is to allow vehicle

2 and vehicle 3 to exchange their estimates $l_{23}(t)$ and $l_{32}(t)$. This way it is possible to project the estimates in such way that $l_{23}(t)l_{32}(t) \neq 4$ and the matrix U is always invertible. The following assumption is made.

Assumption 5. The actual parameters l_{23}^* and l_{32}^* are known to reside in convex compact set Ω_l that does not contain the set $l_{23}^*l_{32}^* = 4$.

Among infinite choices, we can choose an example of Ω_l satisfies $l_{23}^* \geq 0$, $l_{32}^* \geq 0$, $l_{23}^* + l_{32}^* \leq 3.99$ as represented in Figure 4.

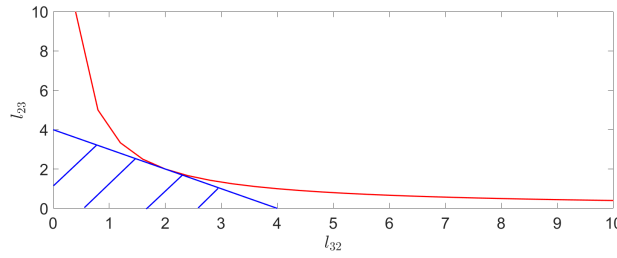


Figure 3-2: Singular set (red curve) and projection set (shaded blue area)

In general, the set Ω_l can be written as

$$\Omega_l = \{l_{23}, l_{32} | g(l_{23}, l_{32}) \leq 0\} \quad (3-6)$$

for some appropriate vector function $g(l_{23}, l_{32})$. The following theorem follows

Theorem 9. Consider a communication graph with cycle described by communication graph in Figure 3-1. The reference model described by (3-1) and for the three agents described by (3-2), the controllers (3-3), and the adaptive laws

$$\begin{aligned} \dot{k}'_{31}(t) &= -\text{sgn}(l_3^*)\gamma b'_m P(e_{31}(t) + e_{32}(t))x_1(t)' \\ \dot{k}'_{32}(t) &= -\text{sgn}(l_3^*)\gamma b'_m P(e_{31}(t) + e_{32}(t))x_2(t)' \\ \dot{k}'_3(t) &= -\text{sgn}(l_3^*)\gamma b'_m P(e_{31}(t) + e_{32}(t))(e_{31}(t) + e_{32}(t))' \\ \dot{l}_{31}(t) &= -\text{sgn}(l_3^*)\gamma b'_m P(e_{31}(t) + e_{32}(t))u_1(t) \\ \dot{l}_{32}(t) &= -\text{sgn}(l_3^*)\gamma b'_m P(e_{31}(t) + e_{32}(t))u_2(t) \\ \dot{k}'_{21}(t) &= -\text{sgn}(l_2^*)\gamma b'_m P(e_{21}(t) + e_{23}(t))x_1(t)' \\ \dot{k}'_{23}(t) &= -\text{sgn}(l_2^*)\gamma b'_m P(e_{21}(t) + e_{23}(t))x_3(t)' \\ \dot{k}'_2(t) &= -\text{sgn}(l_2^*)\gamma b'_m P(e_{21}(t) + e_{23}(t))(e_{21}(t) + e_{23}(t))' \\ \dot{l}_{21}(t) &= -\text{sgn}(l_2^*)\gamma b'_m P(e_{21}(t) + e_{23}(t))u_1(t) \\ \dot{l}_{23}(t) &= -\text{sgn}(l_2^*)\gamma b'_m P(e_{21}(t) + e_{23}(t))u_3(t) \end{aligned} \quad (3-7)$$

with the following modifications

$$\begin{aligned}
\dot{l}_{23}(t) &= \mathbb{P} [-\gamma_l b'_m P(e_{21}(t) + e_{23}(t))u_3(t)] \\
&= \begin{cases} \delta_{l23}(t) & \text{if } l_{23}(t) \in \Omega_l \text{ or } l_{23}(t) \in \delta(\Omega_l) \text{ with } \delta_{l23} \nabla g \leq 0 \\ 0 & \text{otherwise} \end{cases} \\
\dot{l}_{32}(t) &= \mathbb{P} [-\gamma_l b'_m P(e_{31}(t) + e_{32}(t))u_2(t)] \\
&= \begin{cases} \delta_{l32}(t) & \text{if } l_{32}(t) \in \Omega_l \text{ or } l_{32}(t) \in \delta(\Omega_l) \text{ with } \delta_{l32} \nabla g \leq 0 \\ 0 & \text{otherwise} \end{cases}
\end{aligned} \tag{3-8}$$

where \mathbb{P} indicates the projection operator in the set Ω_l , as arising from (3-5). In particular, $\delta(\Omega_l)$ is the border of Ω_l and ∇_g is the derivative of g with respect to l_{23} or l_{32} . Then, we guarantee synchronization of the three agents (3-2) to the reference model (3-1), and the convergence $e_1, e_{21}, e_{23}, e_{31}, e_{32} \rightarrow 0$ for $t \rightarrow \infty$.

Proof. Let us consider the following Lyapunov function

$$\begin{aligned}
V_1(e_1, k_1, l_1) &= e_1' P e_1 + tr\left(\frac{\tilde{k}_1' \tilde{k}_1}{\gamma |l_1^*|}\right) + \frac{\tilde{l}_1^2}{\gamma |l_1^*|} \\
V_2(e_{231}, k_{21}, k_{23}, k_2, l_{21}, l_{23}) &= e_{231}' P e_{231} + tr\left(\frac{\tilde{k}_{21}' \tilde{k}_{21}}{\gamma |l_2^*|}\right) + tr\left(\frac{\tilde{k}_{23}' \tilde{k}_{23}}{\gamma |l_2^*|}\right) + tr\left(\frac{\tilde{k}_2' \tilde{k}_2}{\gamma |l_2^*|}\right) + \frac{\tilde{l}_{21}^2}{\gamma |l_2^*|} + \frac{\tilde{l}_{23}^2}{\gamma |l_2^*|} \\
V_3(e_{321}, k_{31}, k_{32}, k_3, l_{31}, l_{32}) &= e_{321}' P e_{321} + tr\left(\frac{\tilde{k}_{31}' \tilde{k}_{31}}{\gamma |l_3^*|}\right) + tr\left(\frac{\tilde{k}_{32}' \tilde{k}_{32}}{\gamma |l_3^*|}\right) + tr\left(\frac{\tilde{k}_3' \tilde{k}_3}{\gamma |l_3^*|}\right) + \frac{\tilde{l}_{31}^2}{\gamma |l_3^*|} + \frac{\tilde{l}_{32}^2}{\gamma |l_3^*|}
\end{aligned} \tag{3-9}$$

, and follows the same lines as classical adaptive control designs in the presence of parameter projection. In fact, we have

$$\dot{V}_1 + \dot{V}_2 + \dot{V}_3 \leq -e_1' Q e_1 - e_{231}' Q e_{231} - e_{321}' Q e_{321} + V_p \tag{3-10}$$

where

$$V_p(t) \begin{cases} = 0 & \text{if } l_{23}(t), l_{32}(t) \in \Omega_l \text{ or } l_{23}(t) \in \delta(\Omega_l) \text{ with } \delta_{l23} \nabla g \leq 0 \text{ or } l_{32}(t) \in \delta(\Omega_l) \\ & \text{with } \delta_{l32} \nabla g \leq 0 \\ \leq 0 & \text{otherwise} \end{cases} \tag{3-11}$$

i.e V_p is a term that due to convexity of the projection set Ω_l verifies $V_p \leq 0$. Therefore, V_p can only make the derivative of the Lyapunov function more negative [32, Sect 6.6 and 8.5]. Hence,

$$\dot{V}_1 + \dot{V}_2 + \dot{V}_3 \leq -e_1' Q e_1 - e_{231}' Q e_{231} - e_{321}' Q e_{321} \tag{3-12}$$

and stability follows from Barbalat's lemma as in Theorem 9. \square

Remark 7. Theorem 9 basically states that the structure of the network can be exploited to implement appropriate projection laws that make the input well-posed at every time instant, even in the presence of cycles.

3-2 Summary

In this chapter, we have exploited the graph structure to implement appropriate parameter projection and guarantee well-posedness of the actual inputs. The next chapter provides the approach to synchronize the EL systems.

Chapter 4

Adaptive synchronization of uncertain Euler-Lagrange system

This chapter is organized as follows: Section 4-1 introduces the Euler-Lagrange (EL) Systems and inverse dynamic based control. Section 4-2 presents the synchronization of the leader to the reference model. Section 4-3 provides the synchronization of the follower to a neighbor. Please note that the agents are described as EL systems.

4-1 Preliminaries results

4-1-1 Euler-Lagrange systems

The dynamics of a network of EL agents can be described by

$$D_i(q_i)\ddot{q}_i + C_i(q_i, \dot{q}_i)\dot{q}_i + g_i(q_i) = \tau_i, \quad i = \{1, \dots, N\} \quad (4-1)$$

where the term $D_i(q_i)\ddot{q}$ is proportional to the second derivatives of the generalized coordinates, the term $C_i(q_i, \dot{q}_i)\dot{q}$ is the vector of centrifugal/Coriolis forces, proportional to the first derivatives of the generalized coordinates, and the term $g_i(q_i)$ is the vector of potential forces. Finally, the term τ_i represents the external force applied to the system. Throughout this work the following assumptions, standard in literature [33], will be adopted:

Assumption 6. The inertia matrix $D_i(q_i)$ is symmetric positive definite, and both $D_i(q_i)$ and $D_i(q_i)^{-1}$ are uniformly bounded.

Assumption 7. There is an independent control input for each degree of freedom of the system.

Assumption 8. All the parameters of interest such as link masses, moment inertias, etc. appears in the linear-in-the parameter form, i.e. as coefficient of known function of the generalized coordinates.

Remark 8. For most EL agents of practical interests, like robotic manipulators and mobile robots/vehicles, Assumptions 6 and 8 hold [33]. Assumption 7 implies that the system is fully actuated, which is not always the case in practice. For under-actuated EL systems, a control allocator should be put in place to transform the input τ_i into the actual inputs to the system: this will introduce some unmodelled dynamics which can be handled using a modification of the proposed methodology in a robust adaptive sense [34]. While this is a relevant practical aspect, in this work we focus for compactness on fully-actuated EL dynamics.

4-1-2 Inverse dynamic based control

Inverse dynamic based control is a typical control method for EL systems [33], which is here recalled for completeness. Given the dynamics (4-1), the objective of inverse dynamic based control is to cancel all the non-linearities in the system and introduce simple PD control so that the closed-loop system is linear. In the known parameter case, the cancellation of non-linearities can be achieved via the controller

$$\tau_i = D_i(q_i)a_i + C_i(q_i, \dot{q}_i)\dot{q}_i + g_i(q_i) \quad (4-2)$$

where the term a_i is defined as

$$a_i = \ddot{q}^d - K_v \dot{e}_i - K_p e_i \quad (4-3)$$

with $e_i = q_i - q^d$ and K_p , K_v being the proportional and derivative gains of the (multi-variable) PD controller. Note that q^d , \dot{q}^d , and \ddot{q}^d are desired trajectories, velocities, and accelerations to be specified by the user. Substituting (4-2) into (4-1) gives us

$$\begin{aligned} D_i(q_i)(\ddot{q}_i - \ddot{q}^d + K_v \dot{e}_i + K_p e_i) &= 0 \\ \ddot{e}_i + K_v \dot{e}_i + K_p e_i &= 0. \end{aligned} \quad (4-4)$$

The resulting second-order error equation can be written as

$$\begin{bmatrix} \dot{e}_i \\ \ddot{e}_i \end{bmatrix} = \begin{bmatrix} 0 & \mathbf{1} \\ -K_p & -K_v \end{bmatrix} \begin{bmatrix} e_i \\ \dot{e}_i \end{bmatrix} \quad (4-5)$$

or equivalently,

$$\begin{bmatrix} \dot{q}_i \\ \ddot{q}_i \end{bmatrix} = \begin{bmatrix} 0 & \mathbf{1} \\ -K_p & -K_v \end{bmatrix} \begin{bmatrix} q_i \\ \dot{q}_i \end{bmatrix} + \begin{bmatrix} 0 \\ \mathbf{1} \end{bmatrix} (\ddot{q}^d + K_v \dot{q}^d + K_p q^d). \quad (4-6)$$

Remark 9. The closed-loop systems (4-6) is a second-order state-space system whose state matrix must be Hurwitz by construction (by appropriately selecting K_p and K_v). Two things must be noted about (4-2): the first is that the control law (4-2) requires the dynamics to be perfectly known, so as to operate a perfect inversion; the second is that the control law (4-2) requires agent i to know q^d , \dot{q}^d , and \ddot{q}^d . It clear that in practice the dynamics are not known due to parametric uncertainty, leading to imperfect inversion. In addition, in a multi-agent setting, the desired positions, velocities and accelerations may not be available to all systems. In fact, due to communication constraints, it might be impossible to communicate q^d , \dot{q}^d , and \ddot{q}^d to the entire formation, except for a few agents, e.g. the leading agents. Therefore, one cannot implement (4-3) in a distributed way and in the presence of uncertainty. In Section 3, we will design an adaptive distributed version of the inverse dynamic based control, which can be implemented in the presence of uncertainty and use local measurements from neighboring agents.

4-2 Adaptive synchronization of a leader to a reference model

Before giving the main result, let us first consider the communication graph depicted in Figure 4-1. Figure 4-1 provides a simple communication graph where $\mathcal{V} = \{1, 2, 3, 4\}$, $\mathcal{E} = \{(1, 2), (3, 4)\}$, and $\mathcal{T} = \{1, 3\}$. Note that the target nodes will be referred to as leaders in this work, because they can access the information of the pinner: with this directed connection, follower 2 can observe the measurement from leader 1, and follower 4 can observe the measurement from leader 3, but not vice versa. The adjacency matrix

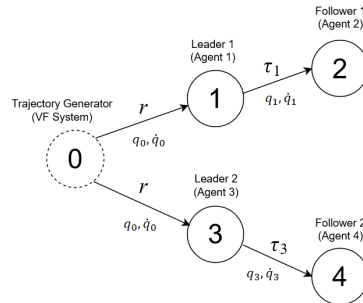


Figure 4-1: Example of multi-agent system communication graph for EL systems.

corresponding to the example in Figure 4-1 is

$$\mathcal{A} = \begin{bmatrix} 0 & 1 & 0 & 0 \\ 0 & 0 & 0 & 0 \\ 0 & 0 & 0 & 1 \\ 0 & 0 & 0 & 0 \end{bmatrix}.$$

In the example of Figure 4-1, we have $\mathcal{M} = [1, 0, 1, 0]'$. In this chapter we will consider hierarchical networks containing a directed spanning tree with the pinner as the root

node. The following problem can be stated.

Problem 1. Given a hierarchical network $\bar{\mathcal{G}}$ of EL heterogeneous uncertain agents (4-1), a pinner with state (q_0, \dot{q}_0) , find a distributed strategy for the inputs τ_i that respects the communication graph, that does not require knowledge of the EL matrices, and that leads to synchronization of the network, i.e. $(q_i, \dot{q}_i) \rightarrow (q_0, \dot{q}_0)$ as $t \rightarrow \infty$, for every agent i .

In this section, we will focus on the control for a leading agent. Because the leading agent has access to q^d , \dot{q}^d , and \ddot{q}^d , the main problem for this agent is to cope with uncertainty. Without loss of generality we denote a leading agent with the index 1: in addition, we focus on a single leading agent because the presence of multiple leaders is a trivial extension of the proposed control law. Let us start by formulating some reference model dynamics

$$\begin{bmatrix} \dot{q}_0 \\ \ddot{q}_0 \end{bmatrix} = \underbrace{\begin{bmatrix} 0 & \mathbb{1} \\ -K_p & -K_v \end{bmatrix}}_{A_m} \underbrace{\begin{bmatrix} q_0 \\ \dot{q}_0 \end{bmatrix}}_{x_m} + \underbrace{\begin{bmatrix} 0 \\ \mathbb{1} \end{bmatrix}}_{B_m} r \quad (4-7)$$

where $q_0, \dot{q}_0 \in \mathbb{R}^n$ is the state of the reference model and $r = \ddot{q}^d + K_v \dot{q}^d + K_p q^d$ is a user-specified reference input. The reference dynamics (4-7) basically represent some homogeneous dynamics all agents should synchronize to. Any leader dynamics in the form (4-2) can be written in the state-space form

$$\begin{bmatrix} \dot{q}_1 \\ \ddot{q}_1 \end{bmatrix} = \underbrace{\begin{bmatrix} 0 & \mathbb{1} \\ 0 & -D_1^{-1} C_1 \end{bmatrix}}_{A_1} \underbrace{\begin{bmatrix} q_1 \\ \dot{q}_1 \end{bmatrix}}_{x_1} + \begin{bmatrix} 0 \\ -D_1^{-1} g_1 \end{bmatrix} + \underbrace{\begin{bmatrix} 0 \\ D_1^{-1} \end{bmatrix}}_{B_1} \tau_1 \quad (4-8)$$

where the dependence of the matrices on q_1, \dot{q}_1 will be omitted whenever obvious. The main idea is to formulate a nonlinear version of the model reference adaptive control method [34, 35], by designing a controller to match the leader dynamics (4-8) to the reference model dynamics (4-7). To this purpose, we propose a controller in the form

$$\tau_1^* = \underbrace{\begin{bmatrix} \bar{K}_1^{*'} & \bar{\bar{K}}_1^{*'} \end{bmatrix}}_{K_1^{*'}} \begin{bmatrix} q_1 \\ \dot{q}_1 \end{bmatrix} + G_1^{*'} + L_1^{*'} r \quad (4-9)$$

where the superscript $*$ indicates an ideal controller whose gains possibly require the knowledge of the system dynamics. The following proposition tells how to find such matching gains.

Proposition 3. There exists an ideal control law in the form of (4-9) that matches the leader dynamics (4-8) to the reference model dynamics (4-7), and whose control gains \bar{K}_1^* , $\bar{\bar{K}}_1^{*'}$, $L_1^{*'}$, and $G_1^{*'}$ are

$$\begin{aligned} \bar{K}_1^{*'} &= -D_1 K_p & L_1^{*'} &= D_1 \\ \bar{\bar{K}}_1^{*'} &= -D_1 K_v + C_1 & G_1^{*'} &= g_1. \end{aligned} \quad (4-10)$$

Proof. By direct substitution of (4-9) into (4-8), we have the leader closed-loop dynamics

$$\begin{bmatrix} \dot{q}_1 \\ \dot{\bar{q}}_1 \end{bmatrix} = \begin{bmatrix} 0 & \mathbb{1} \\ D_1^{-1} \bar{K}_1^{*'} & D_1^{-1} (\bar{K}_1^{*'} - C_1) \end{bmatrix} \begin{bmatrix} q_1 \\ \bar{q}_1 \end{bmatrix} + \begin{bmatrix} 0 \\ -D_1^{-1} (g_1 - G_1^{*'}) \end{bmatrix} + \begin{bmatrix} 0 \\ D_1^{-1} L_1^{*'} \end{bmatrix} r. \quad (4-11)$$

We see that Proposition 3 is verified for the ideal control law

$$\tau_1^* = -D_1 K_p q_1 - D_1 K_v \dot{q}_1 + C_1 \dot{q}_1 + g_1 + D_1 r \quad (4-12)$$

from which we derive the control gains in (4-10). This concludes the proof. \square

Being the system matrices in (4-8) unknown, the controller (4-12) cannot be implemented, and the synchronization task has to be achieved adaptively. Then, inspired by the ideal controller (4-12), we propose the controller

$$\tau_1 = \underbrace{\Theta'_{D_1} \xi_{D_1}}_{\hat{D}_1} (-K_p q_1 - K_v \dot{q}_1 + r) + \underbrace{\Theta'_{C_1} \xi_{C_1}}_{\hat{C}_1} \dot{q}_1 + \underbrace{\Theta'_{g_1} \xi_{g_1}}_{\hat{g}_1} \quad (4-13)$$

where the estimates $\hat{D}_1, \hat{C}_1, \hat{g}_1$ of the ideal matrices have been split in a linear-in-the-parameter form. In fact, in view of Assumption 8, an appropriate linear-in-the-parameter form $D_1 = \Theta'_{D_1} \xi_{D_1}$, $C_1 = \Theta'_{C_1} \xi_{C_1}$ and $g_1 = \Theta'_{g_1} \xi_{g_1}$ can always be found. A specific form of regressand Θ and regressor ξ will be derived later in numerical simulation for the example of Unmanned Aerial Vehicles. Let us define the error $e_1 = x_1 - x_m$, whose dynamics are

$$\begin{aligned} \dot{e}_1 &= A_m e_1 + B_1 (\tilde{\bar{K}}_1' q_1 + \tilde{\bar{K}}_1' \dot{q}_1 + \tilde{G}_1' + \tilde{L}_1' r) \\ &= A_m e_1 + B_1 (\tilde{\Theta}'_{D_1} \xi_{D_1} (-K_p q_1 - K_v \dot{q}_1 + r) + \tilde{\Theta}'_{C_1} \xi_{C_1} \dot{q}_1 + \tilde{\Theta}'_{g_1} \xi_{g_1}) \end{aligned} \quad (4-14)$$

where $\tilde{\bar{K}}_1 = \bar{K}_1 - \bar{K}_1^*$, $\tilde{\bar{K}}_1 = \bar{K}_1 - \bar{K}_1^*$, $\tilde{L}_1 = L_1 - L_1^*$, $\tilde{\Theta}_{D_1} = \Theta_{D_1} - \Theta_{D_1}^*$, $\tilde{\Theta}_{C_1} = \Theta_{C_1} - \Theta_{C_1}^*$ and $\tilde{\Theta}_{g_1} = \Theta_{g_1} - \Theta_{g_1}^*$. The following theorem provides the synchronization result between the leader and the reference model.

Theorem 10. Consider the reference model (4-7), the unknown leader dynamics (4-8), and controller (4-13). Under the assumption that a matrix S_1 exists such that

$$L_1^* S_1 = S_1' L_1^{*'} > 0 \quad (4-15)$$

then, the adaptive laws

$$\begin{aligned} \dot{\Theta}'_{D_1} &= -S_1 B_m' P e_1 (-K_p q_1 - K_v \dot{q}_1 + r)' \xi'_{D_1} \\ \dot{\Theta}'_{C_1} &= -S_1 B_m' P e_1 \dot{q}_1' \xi'_{C_1} \\ \dot{\Theta}'_{g_1} &= -S_1 B_m' P e_1 \xi'_{g_1} \end{aligned} \quad (4-16)$$

where $P = P' > 0$ is such that

$$P A_m + A_m' P = -Q, \quad Q > 0 \quad (4-17)$$

guarantee synchronization of the leader dynamics (4-8) to the reference model (4-7), i.e. $e_1 \rightarrow 0$.

Proof. To analytically show the asymptotic convergence of the synchronization error between the leader and the reference model, let us introduce the following Lyapunov function

$$V_1(e_1, \tilde{\Theta}_{D_1}, \tilde{\Theta}_{C_1}, \tilde{\Theta}_{g_1}) = e_1' P e_1 + \text{tr}(\tilde{\Theta}_{D_1}' S_1^{-1} L_1^{*-1} \tilde{\Theta}_{D_1}) + \text{tr}(\tilde{\Theta}_{C_1}' S_1^{-1} L_1^{*-1} \tilde{\Theta}_{C_1}) + \text{tr}(\tilde{\Theta}_{g_1}' S_1^{-1} L_1^{*-1} \tilde{\Theta}_{g_1}). \quad (4-18)$$

Then it is possible to verify

$$\begin{aligned} \dot{V}_1(e_1, \tilde{\Theta}_{D_1}, \tilde{\Theta}_{C_1}, \tilde{\Theta}_{g_1}) &= e_1' (P A_m + A_m' P) e_1 + 2e_1' P B_1 (\tilde{\Theta}_{D_1}' \xi_{D_1} (-K_p q_1 - K_v \dot{q}_1 + r) \\ &\quad + \tilde{\Theta}_{C_1}' \xi_{C_1} \dot{q}_1 + \tilde{\Theta}_{g_1}' \xi_{g_1}) + 2\text{tr}(\tilde{\Theta}_{D_1}' S_1^{-1} L_1^{*-1} \dot{\tilde{\Theta}}_{D_1}) \\ &\quad + 2\text{tr}(\tilde{\Theta}_{C_1}' S_1^{-1} L_1^{*-1} \dot{\tilde{\Theta}}_{C_1}) + 2\text{tr}(\tilde{\Theta}_{g_1}' S_1^{-1} L_1^{*-1} \dot{\tilde{\Theta}}_{g_1}) \\ &= -e_1' Q e_1 + 2(B_m' P e_1 (-K_p q_1 - K_v \dot{q}_1 + r)' \xi_{D_1}' + \dot{\tilde{\Theta}}_{D_1}' S_1^{-1}) L_1^{*-1} \tilde{\Theta}_{D_1} \\ &\quad + 2(B_m' P e_1 \dot{q}_1' \xi_{C_1}' + \dot{\tilde{\Theta}}_{C_1}' S_1^{-1}) L_1^{*-1} \tilde{\Theta}_{C_1} \\ &\quad + 2(B_m' P e_1 \xi_{g_1}' + \dot{\tilde{\Theta}}_{g_1}' S_1^{-1}) L_1^{*-1} \tilde{\Theta}_{g_1} \\ &= -e_1' Q e_1. \end{aligned} \quad (4-19)$$

Here we used the property $a'b = \text{tr}(b'a)$. From (4-19), we deduce that V_1 has a finite limit, so $e_1, \tilde{\Theta}_{D_1}, \tilde{\Theta}_{C_1}, \tilde{\Theta}_{g_1} \in \mathcal{L}_\infty$. Because $e_1 = x_1 - x_m \in \mathcal{L}_\infty$ and $x_m \in \mathcal{L}_\infty$, we have $x_1 \in \mathcal{L}_\infty$. This implies $x_1, \tilde{\Theta}_{D_1}, \tilde{\Theta}_{C_1}, \tilde{\Theta}_{g_1} \in \mathcal{L}_\infty$. Consequently, we can deduce $\tau_1 \in \mathcal{L}_\infty$. Therefore, all signals in the closed-loop systems are bounded. From (4-19), we can establish that V_1 has a bounded integral, so that we have $e_1 \in \mathcal{L}_2$. Then by using $\tilde{\Theta}_{D_1}, \tilde{\Theta}_{C_1}, \tilde{\Theta}_{g_1}, e_1 \in \mathcal{L}_\infty$, we have $\dot{e}_1 \in \mathcal{L}_\infty$. This concludes the proof of the boundedness of all closed-loop signal and convergence $e_1 \rightarrow 0$ as $t \rightarrow \infty$. \square

Remark 10. Condition (4-15) is mutuited from the well-known condition of multivariable MRAC [36]: even though such condition might sound restrictive because it involves a possibly unknown matrix L_1^* , it can be easily satisfied in most EL systems of practical interests. In fact, in most EL systems like robotic manipulators and mobile robots, the matrix D_i is symmetric in view of some symmetrical geometry of the robot: this implies that L_i^* , even if unknown, is symmetric. Therefore, (4-15) is satisfied by simply selecting $S_i = \gamma I$, for any positive scalar γ .

Remark 11. It is now clear that in the presence of multiple leaders it suffices for each one to implement a control law in the form (4-12) to achieve synchronization to the reference model dynamics (4-7).

4-3 Adaptive synchronization of a follower to a neighbor

In this section we explain how a follower agent that has no access to the desired trajectories q^d , \dot{q}^d , and \ddot{q}^d can still synchronize to the reference model dynamics (4-7) by

exploiting the signals of a neighboring agents for adaptation. By looking at Figure 4-1 and without loss of generality, the follower dynamics are denoted with subscript 2, while the dynamics of the neighboring (hierarchically superior) agent are denoted with subscript 1. The dynamics of any follower in the form (4-2) can be written in the state-space form

$$\begin{bmatrix} \dot{q}_2 \\ \ddot{q}_2 \end{bmatrix} = \underbrace{\begin{bmatrix} 0 & \mathbb{1} \\ 0 & -D_2^{-1}C_2 \end{bmatrix}}_{A_2} \underbrace{\begin{bmatrix} q_2 \\ \dot{q}_2 \end{bmatrix}}_{x_2} + \underbrace{\begin{bmatrix} 0 \\ -D_2^{-1}g_2 \end{bmatrix}}_{B_2} + \underbrace{\begin{bmatrix} 0 \\ D_2^{-1} \end{bmatrix}}_{B_2} \tau_2. \quad (4-20)$$

Analogously to the previous section, we aim to find a matching controller for agent 2: however, since the reference model signals are not available to this agent, we assume the dynamics of the neighboring agent 1 to act as a reference model. Then, let us propose the following controller to match the follower dynamics (4-20) to the leader dynamics (4-8)

$$\tau_2^* = \underbrace{\begin{bmatrix} \bar{K}_{21}^{*'} & \bar{\bar{K}}_{21}^{*'} \end{bmatrix}}_{K_{21}^{*'}} \begin{bmatrix} q_1 \\ \dot{q}_1 \end{bmatrix} + \underbrace{\begin{bmatrix} \bar{K}_2^{*'} & \bar{\bar{K}}_2^{*'} \end{bmatrix}}_{K_2^{*'}} \underbrace{\begin{bmatrix} q_2 - q_1 \\ \dot{q}_2 - \dot{q}_1 \end{bmatrix}}_{e_{21}} + G_2^{*'} + L_{21}^{*'} \tau_1. \quad (4-21)$$

The following proposition explains how to find the matching control gains in (4-21).

Proposition 4. There exists an ideal control law in the form (4-21) that matches the follower dynamics (4-20) to the leader dynamics (4-8), and whose gains $\bar{K}_2^{*'}, \bar{\bar{K}}_2^{*'}, \bar{K}_{21}^{*'}, \bar{\bar{K}}_{21}^{*'}, L_{21}^{*'},$ and $G_2^{*'}$ are

$$\begin{aligned} \bar{K}_2^{*'} &= -D_2 K_p & \bar{K}_{21}^{*'} &= 0 & G_2^{*'} &= g_2 \\ \bar{\bar{K}}_2^{*'} &= -D_2 K_v + C_2 & \bar{\bar{K}}_{21}^{*'} &= C_2 - D_2 D_1^{-1} C_1 & L_{21}^{*'} &= D_2 D_1^{-1}. \end{aligned} \quad (4-22)$$

Proof. By direct substitution of (4-21) into (4-20), we have the leader closed-loop dynamics

$$\begin{aligned} \begin{bmatrix} \dot{q}_2 \\ \ddot{q}_2 \end{bmatrix} &= \begin{bmatrix} 0 & \mathbb{1} \\ D_2^{-1} \bar{K}_2^{*'} & D_2^{-1}(\bar{\bar{K}}_2^{*'} - C_2) \end{bmatrix} \begin{bmatrix} q_2 \\ \dot{q}_2 \end{bmatrix} + \begin{bmatrix} 0 & 0 \\ D_2^{-1}(\bar{K}_{21}^{*'} - \bar{K}_2^{*'}) & D_2^{-1}(\bar{\bar{K}}_{21}^{*'} - \bar{\bar{K}}_2^{*'}) \end{bmatrix} \begin{bmatrix} q_1 \\ \dot{q}_1 \end{bmatrix} \\ &+ \begin{bmatrix} 0 \\ -D_2^{-1}(-g_2 + G_2^{*'}) \end{bmatrix} + \begin{bmatrix} 0 \\ D_2^{-1} L_{21}^{*'} \end{bmatrix} \tau_1 \end{aligned} \quad (4-23)$$

from which we see that matching is achieved for the ideal control law

$$\begin{aligned} \tau_2^* &= C_2 \dot{q}_1 - D_2 D_1^{-1} C_1 \dot{q}_1 - D_2 K_p \bar{e}_{21} - D_2 K_v \bar{\bar{e}}_{21} + C_2 \bar{\bar{e}}_{21} + g_2 + D_2 D_1^{-1} \tau_1 \\ &= C_2 \dot{q}_2 + D_2 D_1^{-1} \tau_1 - D_2 D_1^{-1} C_1 \dot{q}_1 - D_2 (K_p \bar{e}_{21} + K_v \bar{\bar{e}}_{21}) + g_2 \end{aligned} \quad (4-24)$$

where we have defined $\bar{e}_{21} = q_2 - q_1$, $\bar{\bar{e}}_{21} = \dot{q}_2 - \dot{q}_1$. From (4-24) we find the control gains (4-22). This concludes the proof. \square

Remark 12. Differently from Proposition 4, which gives us matching conditions between an agent and the reference model dynamics, Proposition 2 gives us matching conditions among neighboring agent. In fact, it is easy to show how (4-24) implies the existence of coupling gains \bar{K}_{21}^* , $\bar{\bar{K}}_{21}^*$, L_{21}^* satisfying

$$\begin{aligned}\bar{K}_{21}^* &= \bar{K}_2^* - L_{21}^* \bar{K}_1^* \\ \bar{\bar{K}}_{21}^* &= \bar{\bar{K}}_2^* - L_{21}^* \bar{\bar{K}}_1^* \\ L_{21}^* &= L_2^* (L_1^*)^{-1}\end{aligned}\tag{4-25}$$

where $L_2^* = D_2$. Therefore, Proposition 2 can be interpreted as a distributed matching condition among neighboring agents.

Being the system matrices in (4-20) unknown, the control (4-24) cannot be implemented, and the synchronization task has to be achieved adaptively. Then, inspired by the ideal controller (4-24), we propose the controller

$$\begin{aligned}\tau_2 &= - \underbrace{\Theta'_{D_2} \xi_{D_2}}_{\hat{D}_2} (K_p \bar{e}_{21} + K_v \bar{\bar{e}}_{21}) + \underbrace{\Theta'_{C_2} \xi_{C_2}}_{\hat{C}_2} \dot{q}_2 + \underbrace{\Theta'_{D_2 D_1} \xi_{D_2 D_1}}_{\widehat{D_2 D_1}} \tau_1 - \underbrace{\Theta'_{D_2 D_1 C_1} \xi_{D_2 D_1 C_1}}_{\widehat{D_2 D_1 C_1}} \dot{q}_1 \\ &\quad + \underbrace{\Theta'_{g_2} \xi_{g_2}}_{\hat{g}_2}\end{aligned}\tag{4-26}$$

where the estimates \hat{D}_2 , \hat{C}_2 , $\widehat{D_2 D_1}$, $\widehat{D_2 D_1 C_1}$, \hat{g}_2 of the ideal matrices have been split in a linear-in-the-parameter form, in view of Assumption 8. In fact, Assumption 8 guarantees $D_2 = \Theta_{D_2}^* \xi_{D_2}$, $C_2 = \Theta_{C_2}^* \xi_{C_2}$, $g_2 = \Theta_{g_2}^* \xi_{g_2}$, $D_2 D_1 = \Theta_{D_2 D_1}^* \xi_{D_2 D_1}$ and $D_2 D_1 C_1 = \Theta_{D_2 D_1 C_1}^* \xi_{D_2 D_1 C_1}$: again, a specific form of regressand Θ and regressor ξ will be revealed in Section 5 for the example of Unmanned Aerial Vehicles. Let us define the error $e_{21} = x_2 - x_1$, whose dynamics are

$$\begin{aligned}\dot{e}_{21} &= A_m e_{21} + B_2 (\tilde{K}_2' e_{21} + \tilde{K}_{21}' x_1 + \tilde{L}_{21}' \tau_1 + \tilde{G}_2') \\ &= A_m e_{21} + B_2 (\tilde{\bar{K}}_2' \bar{e}_{21} + \tilde{\bar{K}}_{21}' \bar{\bar{e}}_{21} + \tilde{\bar{K}}_{21}' q_1 + \tilde{\bar{K}}_{21}' \dot{q}_1 + \tilde{L}_{21}' \tau_1 + \tilde{G}_2') \\ &= A_m e_{21} + B_2 (\tilde{\Theta}'_{C_2} \xi_{C_2} \dot{q}_2 + \tilde{\Theta}'_{D_2 D_1} \xi_{D_2 D_1} \tau_1 - \tilde{\Theta}'_{D_2 D_1 C_1} \xi_{D_2 D_1 C_1} \dot{q}_1 \\ &\quad - \tilde{\Theta}'_{D_2} \xi_{D_2} (K_p \bar{e}_{21} + K_v \bar{\bar{e}}_{21}) + \tilde{\Theta}'_{g_2} \xi_{g_2})\end{aligned}\tag{4-27}$$

where $\tilde{K}_2 = K_2 - K_2^*$, $\tilde{K}_{21} = K_{21} - K_{21}^*$, $\tilde{L}_{21} = L_{21} - L_{21}^*$, $\tilde{\Theta}_{D_2} = \Theta_{D_2} - \Theta_{D_2}^*$, $\tilde{\Theta}_{C_2} = \Theta_{C_2} - \Theta_{C_2}^*$, $\tilde{\Theta}_{g_2} = \Theta_{g_2} - \Theta_{g_2}^*$, $\tilde{\Theta}_{D_2 D_1} = \Theta_{D_2 D_1} - \Theta_{D_2 D_1}^*$ and $\tilde{\Theta}_{D_2 D_1 C_1} = \Theta_{D_2 D_1 C_1} - \Theta_{D_2 D_1 C_1}^*$. The following theorem provides the follower-leader synchronization.

Theorem 11. Consider the reference model (4-7), the unknown leader dynamics (4-8), the unknown follower dynamics (4-20), and controller (4-26). Provided that there exists a matrix S_2 such that

$$L_2 S_2 = S_2' L_2' > 0\tag{4-28}$$

then, the adaptive laws

$$\begin{aligned}\dot{\Theta}'_{C_2} &= -S_2 B'_m P e_{21} \dot{q}'_2 \xi'_{C_2} & \dot{\Theta}'_{D_2} &= S_2 B'_m P e_{21} (K_p \bar{e}_{21} + K_v \bar{\bar{e}}_{21})' \xi'_{D_2} \\ \dot{\Theta}'_{D_2 D_1} &= -S_2 B'_m P e_{21} \tau'_1 \xi'_{D_2 D_1} & \dot{\Theta}'_{g_2} &= -S_2 B'_m P e_{21} \xi'_{g_2} \\ \dot{\Theta}'_{D_2 D_1 C_1} &= S_2 B'_m P e_{21} \dot{q}'_1 \xi'_{D_2 D_1 C_1}\end{aligned}\tag{4-29}$$

where $P = P' > 0$ is such that (4-17) holds, guarantee synchronization of the follower dynamics (4-20) to the leader dynamics (4-8), i.e. $e_{21} \rightarrow 0$.

Proof. To analytically show the asymptotic convergence of the synchronization error between the follower and the leader, let us introduce the following Lyapunov function

$$\begin{aligned}V_2 &= e'_{21} P e_{21} + tr(\tilde{\Theta}'_{C_2} S_2^{-1} L_2^{*-1} \tilde{\Theta}_{C_2}) + tr(\tilde{\Theta}'_{D_2 D_1} S_2^{-1} L_2^{*-1} \tilde{\Theta}_{D_2 D_1}) \\ &\quad + tr(\tilde{\Theta}'_{D_2 D_1 C_1} S_2^{-1} L_2^{*-1} \tilde{\Theta}_{D_2 D_1 C_1}) + tr(\tilde{\Theta}'_{D_2} S_2^{-1} L_2^{*-1} \tilde{\Theta}_{D_2}) + tr(\tilde{\Theta}'_{g_2} S_2^{-1} L_2^{*-1} \tilde{\Theta}_{g_2}).\end{aligned}\tag{4-30}$$

Then it is possible to verify

$$\begin{aligned}\dot{V}_2 &= -e'_{21} Q e_{21} + 2e'_{21} P B_2 (\tilde{\Theta}'_{C_2} \xi_{C_2} \dot{q}_2 + \tilde{\Theta}'_{D_2 D_1} \xi_{D_2 D_1} \tau_1 - \tilde{\Theta}'_{D_2 D_1 C_1} \xi_{D_2 D_1 C_1} \dot{q}_1 \\ &\quad - \tilde{\Theta}'_{D_2} \xi_{D_2} (K_p \bar{e}_{21} + K_v \bar{\bar{e}}_{21}) + \tilde{\Theta}'_{g_2} \xi_{g_2}) + 2tr(\tilde{\Theta}'_{C_2} S_2^{-1} L_2^{*-1} \dot{\tilde{\Theta}}_{C_2}) + 2tr(\tilde{\Theta}'_{D_2} S_2^{-1} L_2^{*-1} \dot{\tilde{\Theta}}_{D_2}) \\ &\quad + 2tr(\tilde{\Theta}'_{D_2 D_1} S_2^{-1} L_2^{*-1} \dot{\tilde{\Theta}}_{D_2 D_1}) + 2tr(\tilde{\Theta}'_{D_2 D_1 C_1} S_2^{-1} L_2^{*-1} \dot{\tilde{\Theta}}_{D_2 D_1 C_1}) + 2tr(\tilde{\Theta}'_{g_2} S_2^{-1} L_2^{*-1} \dot{\tilde{\Theta}}_{g_2}) \\ &= -e'_{21} Q e_{21} + 2(B'_m P e_{21} \dot{q}'_2 \xi'_{C_2} + \dot{\tilde{\Theta}}'_{C_2} S_2^{-1}) L_2^{*-1} \tilde{\Theta}_{C_2} + 2(B'_m P e_{21} \xi'_{g_2} + \dot{\tilde{\Theta}}'_{g_2} S_2^{-1}) L_2^{*-1} \tilde{\Theta}_{g_2} \\ &\quad + 2(B'_m P e_{21} \tau'_1 \xi'_{D_2 D_1} + \dot{\tilde{\Theta}}'_{D_2 D_1} S_2^{-1}) L_2^{*-1} \tilde{\Theta}_{D_2 D_1} \\ &\quad - 2(B'_m P e_{21} \dot{q}'_1 \xi'_{D_2 D_1 C_1} + \dot{\tilde{\Theta}}'_{D_2 D_1 C_1} S_2^{-1}) L_2^{*-1} \tilde{\Theta}_{D_2 D_1 C_1} \\ &\quad - 2(B'_m P e_{21} (K_p \bar{e}_{21} + K_v \bar{\bar{e}}_{21})' \xi'_{D_2} + \dot{\tilde{\Theta}}'_{D_2} S_2^{-1}) L_2^{*-1} \tilde{\Theta}_{D_2} \\ &= -e'_{21} Q e_{21}.\end{aligned}\tag{4-31}$$

Following similar steps as in the proof of Theorem 10, from (4-31) we deduce that V_2 has a finite limit, so $e_2, \tilde{\Theta}_{C_2}, \tilde{\Theta}_{D_2 D_1}, \tilde{\Theta}_{D_2 D_1 C_1}, \tilde{\Theta}_{D_2}, \tilde{\Theta}_{g_2} \in \mathcal{L}_\infty$. Because $e_{21} = x_2 - x_1 \in \mathcal{L}_\infty$ and $x_1 \in \mathcal{L}_\infty$, we have $x_2 \in \mathcal{L}_\infty$. This implies $x_2, \tilde{\Theta}_{C_2}, \tilde{\Theta}_{D_2 D_1}, \tilde{\Theta}_{D_2 D_1 C_1}, \tilde{\Theta}_{D_2}, \tilde{\Theta}_{g_2} \in \mathcal{L}_\infty$. Consequently, we can deduce $\tau_2 \in \mathcal{L}_\infty$. Therefore, all signals in the closed-loop systems are bounded. From (4-31), we can establish that V_2 has a bounded integral, so that we have $e_{21} \in \mathcal{L}_2$. Then by using $\tilde{\Theta}_{C_2}, \tilde{\Theta}_{D_2 D_1}, \tilde{\Theta}_{D_2 D_1 C_1}, \tilde{\Theta}_{D_2}, \tilde{\Theta}_{g_2}, e_{21} \in \mathcal{L}_\infty$, we have $\dot{e}_{21} \in \mathcal{L}_\infty$. This concludes the proof of the boundedness of all closed-loop signal and convergence $e_{21} \rightarrow 0$ as $t \rightarrow \infty$. \square

Remark 13. It is worth remarking that the controller (4-26) and the adaptive law (4-29) do not require the knowledge of the desired trajectories q^d, \dot{q}^d , and \ddot{q}^d . On the other hand, local information from the neighboring agent 1 is needed to agent 2, namely

the state q_1, \dot{q}_1 and the input τ_1 . Now, comparing controller (4-26) with [37, 38] or similar approaches, we see that the proposed protocol is essentially simpler, because it does not require an extra dynamical system to exchange in a distributed manner the observer variables and reconstruct the leader's signal: therefore, the distributed observer mechanism has been replaced with local exchange of input information among neighbors.

4-3-1 Extension to acyclic graphs

At this point we have shown that the proposed theory is consistent, modulo the nonlinear setting, with the theory in [25]. Therefore, it is not difficult to extend the results of Theorems 10 and 11 to hierarchical communication graphs. Only the main points are given for lack of space. Except for the leaders, which use controller (4-13) and adaptive laws (4-16), the following controller is proposed for the other agents

$$\begin{aligned} \tau_j = & -\frac{\sum_{i=1}^N a_{ij} \hat{D}_j (K_p(q_j - q_i) + K_v(\dot{q}_j - \dot{q}_i))}{\sum_{i=1}^N a_{ij}} + \frac{\sum_{i=1}^N a_{ij} \hat{C}_j \dot{q}_j}{\sum_{i=1}^N a_{ij}} + \frac{\sum_{i=1}^N a_{ij} \widehat{D_j D_i} \tau_i}{\sum_{i=1}^N a_{ij}} \\ & - \frac{\sum_{i=1}^N a_{ij} \widehat{D_j D_i} \hat{C}_i \dot{q}_i}{\sum_{i=1}^N a_{ij}} + \frac{\sum_{i=1}^N a_{ij} \hat{g}_j}{\sum_{i=1}^N a_{ij}} \end{aligned} \quad (4-32)$$

where the terms a_{ij} indicate the entries of the adjacency matrix \mathcal{A} and of the target vector \mathcal{M} , as explained in Section 2.3 (one can verify that, with the appropriate adjacency matrices, the adaptive controller (4-32) reduces to the special case (4-26)). The following result holds.

Theorem 12. Consider the unknown EL agents (4-1), with reference model (4-7), controllers (4-13), (4-32), and adaptive laws (4-16) and

$$\begin{aligned} \dot{\Theta}'_{D_j} &= S_j B'_m P \left[\sum_{i=1}^N a_{ij} (x_j - x_i) \right] \left[\sum_{i=1}^N a_{ij} (K_p(q_j - q_i) + K_v(\dot{q}_j - \dot{q}_i))' \xi'_{D_j D_i} \right] \\ \dot{\Theta}'_{D_j D_i} &= -S_j B'_m P \left[\sum_{i=1}^N a_{ij} (x_j - x_i) \right] \left[\sum_{i=1}^N a_{ij} \tau_i' \xi'_{D_j D_i} \right] \\ \dot{\Theta}'_{C_j} &= -S_j B'_m P \left[\sum_{i=1}^N a_{ij} (x_j - x_i) \right] \dot{q}_j' \xi'_{C_j} \\ \dot{\Theta}'_{D_j D_i C_i} &= S_j B'_m P \left[\sum_{i=1}^N a_{ij} (x_j - x_i) \right] \left[\sum_{i=1}^N a_{ij} \dot{q}_i' \xi'_{D_j D_i C_i} \right] \\ \dot{\Theta}'_{g_j} &= -S_j B'_m P \left[\sum_{i=1}^N a_{ij} (x_j - x_i) \right] \xi'_{g_j} \end{aligned} \quad (4-33)$$

where Θ_{C_j} , $\Theta_{D_j D_i}$, $\Theta_{D_j D_i C_i}$, Θ_{D_j} , Θ_{g_j} are the estimate of the regressand of C_j , $D_j D_i$, $D_j D_i C_i$, D_j , g_j respectively. Then, all closed-loop signals are bounded and, for any (i, j)

such that $a_{ij} \neq 0$, we have $e_{ji} = x_j - x_i \rightarrow 0$ as $t \rightarrow \infty$. In addition, for every agent j we have $e_j = x_j - x_m \rightarrow 0$ as $t \rightarrow \infty$.

Proof. Let us adopt similar tools as Theorems 10 and 11 by considering the distributed Lyapunov function

$$\begin{aligned} V_j = & \sum_{j=1}^N \left[\sum_{i=0}^N a_{ij} e_{ji} \right]' P \left[\sum_{i=0}^N a_{ij} e_{ji} \right] + \sum_{j=1}^N a_{ij} \text{tr} \left[\tilde{\Theta}'_{C_j} S_j^{-1} L_j^{*-1} \tilde{\Theta}_{C_j} \right] \\ & + \sum_{j=1}^N \sum_{i=1}^N a_{ij} \text{tr} \left[\tilde{\Theta}'_{D_j D_i} S_j^{-1} L_j^{*-1} \tilde{\Theta}_{D_j D_i} \right] + \sum_{j=1}^N \sum_{i=1}^N a_{ij} \text{tr} \left[\tilde{\Theta}'_{D_j D_i C_i} S_j^{-1} L_j^{*-1} \tilde{\Theta}_{D_j D_i C_i} \right] \\ & + \sum_{j=1}^N \sum_{i=1}^N a_{ij} \text{tr} \left[\tilde{\Theta}'_{D_j} S_j^{-1} L_j^{*-1} \tilde{\Theta}_{D_j} \right] + \sum_{j=1}^N \sum_{i=1}^N a_{ij} \text{tr} \left[\tilde{\Theta}'_{g_j} S_j^{-1} L_j^{*-1} \tilde{\Theta}_{g_j} \right] \end{aligned} \quad (4-34)$$

where the index $i = 0$ is used for the reference model, i.e. $e_{j0} = e_j = x_j - x_m$. Let us define $\bar{e}_{ji} = q_j - q_i$ and $\bar{e}_{ji} = \dot{q}_j - \dot{q}_i$. Then, from (4-1) and (4-32), we obtain the following error dynamics

$$\begin{aligned} \dot{e}_{ji} = & A_m e_{ji} + B_j (\tilde{K}_j' e_{ji} + \tilde{K}_{ji}' x_i + \tilde{L}_{ji}' \tau_i + \tilde{G}_j') \\ = & A_m e_{ji} + B_j (\tilde{\Theta}'_{C_j} \xi_{C_j} \dot{q}_j + \tilde{\Theta}'_{D_j D_i} \xi_{D_j D_i} \tau_i - \tilde{\Theta}'_{D_j D_i C_i} \xi_{D_j D_i C_i} \dot{q}_i \\ & - \tilde{\Theta}'_{D_j} \xi_{D_j} (K_p \bar{e}_{ji} + K_v \bar{e}_{ji}) + \tilde{\Theta}'_{g_j} \xi_{g_j}). \end{aligned} \quad (4-35)$$

Clearly, we have a similar structure as in the previously developed two-agent case. Then, it is possible to verify that

$$\begin{aligned} \dot{V}_j = & - \sum_{j=1}^N \left[\sum_{i=0}^N a_{ij} e_{ji} \right]' Q \left[\sum_{i=0}^N a_{ij} e_{ji} \right] + 2 \left[\sum_{i=0}^N a_{ij} e_{ji} \right]' P b_j \left[\sum_{j=1}^N a_{ij} \tilde{\Theta}'_{C_j} \xi_{C_j} \dot{q}_j \right. \\ & + \sum_{j=1}^N a_{ij} \tilde{\Theta}'_{D_j D_i} \xi_{D_j D_i} \tau_i - \sum_{j=1}^N a_{ij} \tilde{\Theta}'_{D_j D_i C_i} \xi_{D_j D_i C_i} \dot{q}_i - \sum_{j=1}^N a_{ij} \tilde{\Theta}'_{D_j} \xi_{D_j} (K_p \bar{e}_{ji} + K_v \bar{e}_{ji}) \\ & + \sum_{j=1}^N a_{ij} \tilde{\Theta}'_{g_j} \xi_{g_j} \left. \right] + 2 \sum_{j=1}^N a_{ij} \text{tr} \left[\tilde{\Theta}'_{C_j} S_j^{-1} L_j^{*-1} \dot{\tilde{\Theta}}_{C_j} \right] + 2 \sum_{j=1}^N a_{ij} \text{tr} \left[\tilde{\Theta}'_{g_j} S_j^{-1} L_j^{*-1} \dot{\tilde{\Theta}}_{g_j} \right] \\ & + 2 \sum_{j=1}^N \sum_{i=1}^N a_{ij} \text{tr} \left[\tilde{\Theta}'_{D_j D_i C_i} S_j^{-1} L_j^{*-1} \dot{\tilde{\Theta}}_{D_j D_i C_i} \right] + 2 \sum_{j=1}^N a_{ij} \text{tr} \left[\tilde{\Theta}'_{D_j} S_j^{-1} L_j^{*-1} \dot{\tilde{\Theta}}_{D_j} \right] \\ & + 2 \sum_{j=1}^N \sum_{i=1}^N a_{ij} \text{tr} \left[\tilde{\Theta}'_{D_j D_i} S_j^{-1} L_j^{*-1} \dot{\tilde{\Theta}}_{D_j D_i} \right] \\ = & - \sum_{j=1}^N \left[\sum_{i=0}^N a_{ij} e_{ji} \right]' Q \left[\sum_{i=0}^N a_{ij} e_{ji} \right]. \end{aligned} \quad (4-36)$$

This can be used to derive boundedness of all closed-loop signals and convergence of e_{ji} to zero, which can be proved by using the Barbalat's Lemma procedure already adopted in Theorems 10 and 11. Convergence of $x_j - x_m$ to zero follows according to [29] by using the hierarchical structure of the graph. This concludes the proof. \square

Remark 14. All the synchronization results have been given for errors in the form $e_{ji} = x_j - x_i$. This implies that upon synchronization all the agents will converge to a common trajectory depending on the desired trajectories q^d , \dot{q}^d , and \ddot{q}^d , and on the reference model dynamics K_p and K_v . It is not difficult to show that the proposed synchronization protocol can be extended to include formation gaps, provided that the error

$$e_{ji} = x_j - x_i + d_{ji} = \begin{bmatrix} q_j \\ \dot{q}_j \end{bmatrix} - \begin{bmatrix} q_i \\ \dot{q}_i \end{bmatrix} + \begin{bmatrix} \bar{d}_{ji} \\ 0 \end{bmatrix} \quad (4-37)$$

is considered, where d_{ji} contains the desired formation displacement \bar{d}_{ji} among agents j and i . Crucial to this extension is the fact that

$$\begin{bmatrix} 0 & \mathbf{1} \\ 0 & -D_i^{-1}C_i \end{bmatrix} \begin{bmatrix} \bar{d}_{ji} \\ 0 \end{bmatrix} = \begin{bmatrix} 0 \\ 0 \end{bmatrix} \quad (4-38)$$

implying that the added displacement does not contribute to the error dynamics. Defining the formation as a desired set of displacements is the standard way most formations are defined, e.g. vehicle formations or other robotic formations [39, 40].

4-3-2 Summary

The proposed distributed adaptive control have been derived to synchronize uncertain heterogeneous Euler-Lagrange systems. The proposed control algorithm is distributed among the agent and utilizes local state and input information, without any extra auxiliary variables nor sliding modes. The stability of the proposed controlled was derived analytically by introducing an appropriately defined distributed Lyapunov function.

Chapter 5

Numerical simulations

This chapter is organized as follows: Section 5-1 presents the simulation of output-feedback MRAC with switching topologies restricted to DAG. Section 5-2 presents the simulation of state-feedback MRAC with switching topologies and the capability to handle a cycle. Section 5-3 presents the simulation of a formation of Unmanned Aerial Vehicles (UAVs).

5-1 Output-feedback MRAC: Yaw attitude control of multi UAV

Before giving the numerical simulation, it is functional to discuss the switching adaptive control scheme. communication losses between agents and a certain purpose of the MASs may lead to the changing of topology. By using the proposed adaptive distributed control based on MRAC, one can handle the switching topologies via multiple switched adaptive control. The switching algorithm is based on the number of the predecessor of an agent. Let us consider the switching adaptive controller scheme for the agent $k \in \{2, 3, \dots, N\}$ where N is the last agent in the graph and $i \in \mathbb{N}_k$, where \mathbb{N}_k is the neighbors of the agent k as in Figure 5-1. The activation of one or of the other controller depends on the switching logic σ which is based on the number of neighbors. Also, note that the learning process should be stopped when the controller is inactive and reinitialized once the controller is active.

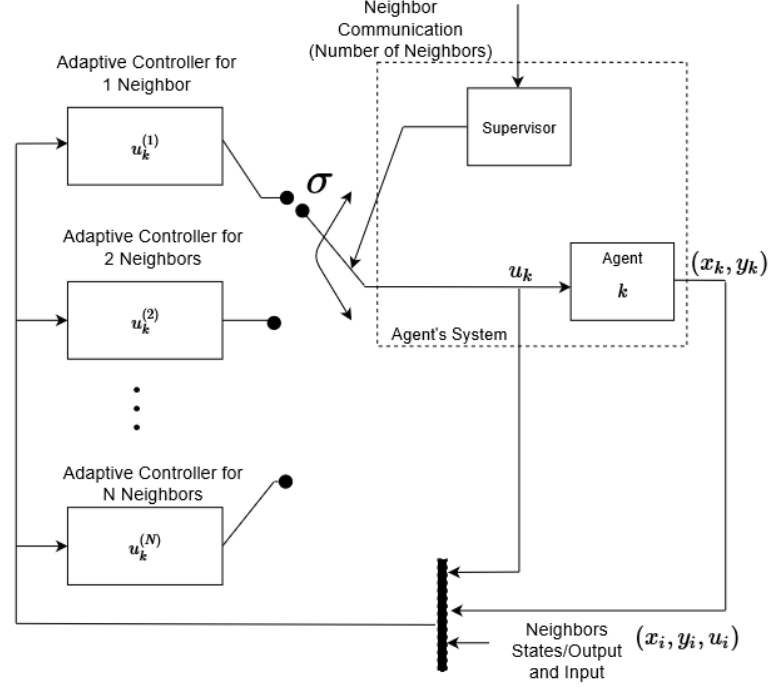


Figure 5-1: The switching adaptive control for agent k

However, such a dwell time is unknown in the output-feedback case. Therefore, in this work we are proposing an adaptive switching scheme and evaluating its effectiveness in simulations. The switching scheme resembles the multiple model adaptive control, e.g., as discussed in [41–43]. In line with [44, 45], some simplified quadcopter dynamics are used as a numerical example. The simplified quadcopter attitude dynamics is given as follows:

$$\ddot{\psi} = I_y^{-1} \tau_\psi \quad (5-1)$$

where ψ , I_y , and τ_ψ are the yaw angle, the rotational moments of inertia on the y-axis, and the rotating torque on yaw angle, respectively. The yaw angle output will be utilized to synchronize the yaw angle for all the agents. The state-space representation of the quadcopter i with attitude dynamics:

$$\begin{aligned} \dot{x}_{\psi i} &= \begin{bmatrix} 0 & 1 \\ 0 & 0 \end{bmatrix} x_{\psi i} + \begin{bmatrix} 0 \\ I_{yi}^{-1} \end{bmatrix} \tau_\psi \\ y_{\psi i} &= \begin{bmatrix} 1 & 0 \end{bmatrix} x_{\psi i} \end{aligned} \quad (5-2)$$

where the state vector, $x_{\psi i} = [\psi_i, \dot{\psi}_i]$, comprises the yaw angle and the yaw rate, $i \in \{1, \dots, N\}$, where N is the total number of the quadcopter. Note that (5-2) has relative degree 2 ($n^* = 2$). Index 1 indicates the leader quadcopter, which is the only quadcopter that has direct access to the reference model. The reference model is indicated as

fictitious Agent 0, which can communicate the reference signal to Agent 1. The reference model dynamics in state-space formulation is given as follows:

$$\begin{aligned}\dot{x}_{\psi m} &= \begin{bmatrix} 0 & 1 \\ \alpha_1 & \alpha_2 \end{bmatrix} x_{\psi m} + \begin{bmatrix} 0 \\ I_{ym}^{-1} \end{bmatrix} \tau_{\psi} \\ y_{\psi m} &= \begin{bmatrix} 1 & 0 \end{bmatrix} x_{\psi m}\end{aligned}\quad (5-3)$$

where the model reference parameters are taken as: $\alpha_1 = -0.5, \alpha_2 = -1, I_{ym} = 1$, and the initial condition of the reference model $[\psi_i, \dot{\psi}_i] = [1, -1]$. Each quadcopter has different and unknown rotational moments of inertia I_y , and the initial state is also unknown. Therefore, the network is composed of heterogeneous and unknown agents. Table 5-3 shows the parameters of each quadcopter that are used only to simulate the network.

Table 5-1: Quadcopter parameters and initial conditions.

	I_{yi}	$[\psi_i, \dot{\psi}_i]$
Quadcopter 1	1	$[1, 1]$
Quadcopter 2	3	$[-1, -1]$
Quadcopter 3	2	$[-1, 0]$
Quadcopter 4	4	$[0, 1]$
Quadcopter 5	0.5	$[1, 0]$
Quadcopter 6	0.75	$[-1, 1]$

The simulations for multi-agent output-feedback MRAC with switching topology are carried out on the directed graph shown in Figure 5-2. The communication between Node 4 and Node 1 varies with time, e.g., due to communication losses. It must be noted that Agent 4 only has one parent neighbor if the edge is inactive and has two parents if the edge is active.

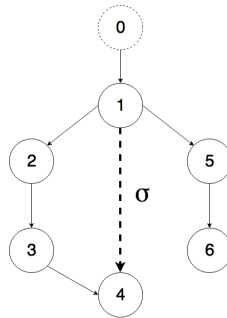


Figure 5-2: The directed communication graph output-feedback scheme with switching topology.

The design parameters are taken as $F = -0.7$, $\rho = 0.3$, and all coupling vector gains are initialized to be 0. Let us define the adaptive gain Γ_i for each agent i as follows:

$$\begin{aligned}\Gamma_1 &= \text{diag}\{\Gamma_l, \Gamma_f, \Gamma_g, \Gamma_c\} \\ \Gamma_2 &= \Gamma_3 = \Gamma_5 = \Gamma_6 = \text{diag}\{\Gamma_l, \Gamma_f, \Gamma_g, \Gamma_c, \Gamma_l, \Gamma_f, \Gamma_g\} \\ \Gamma_4 &= \text{diag}\{\Gamma_l, \Gamma_f, \Gamma_g, \Gamma_c, \Gamma_l, \Gamma_f, \Gamma_g, \Gamma_c, \Gamma_l, \Gamma_f, \Gamma_g\}\end{aligned}\quad (5-4)$$

Γ have been selected to give a smooth response and acceptable input action where $\Gamma_l = 0.2$, $\Gamma_f = 0.05$, $\Gamma_g = 0.1$, and $\Gamma_c = 0.025$. In our case, two reference inputs are considered:

1. a constant reference input with an amplitude of 1.
2. a sinusoidal reference input with a frequency of 0.2 rad/s and an amplitude of 1.

The activity or inactivity of the edge is defined by the switching edge of Figure 5-2 ($\sigma = 1$, edge is active and $\sigma = 0$, edge is inactive). The switching edge signal is shown in Figure 5-3. If the controller is not switching, Agent 4 continues to use the controller for two neighbors instead of only one. Note that the parameters of Agent 1 are equal to zero when there is no connection.

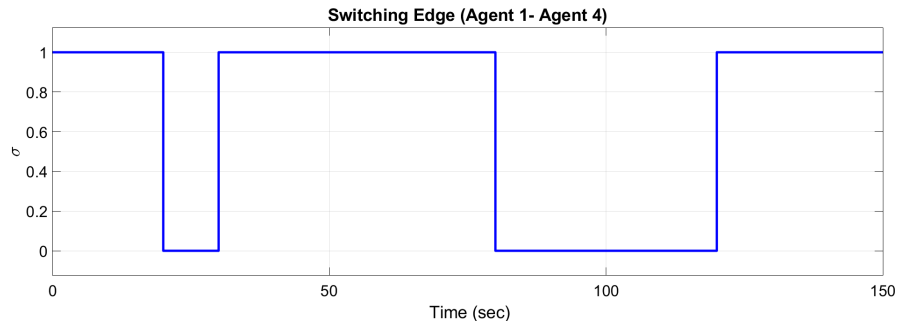
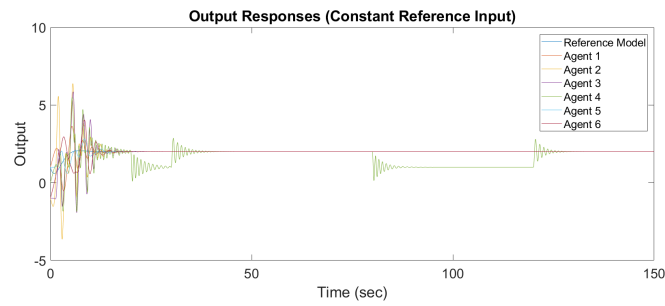
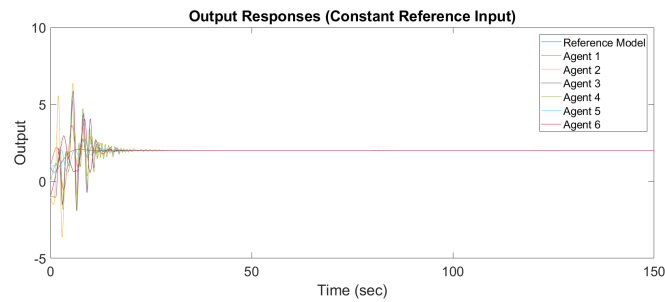


Figure 5-3: Switching edge σ .

The output response of synchronization with a constant reference input and a sinusoidal reference input are shown in Figures 5-4 and 5-5, respectively.

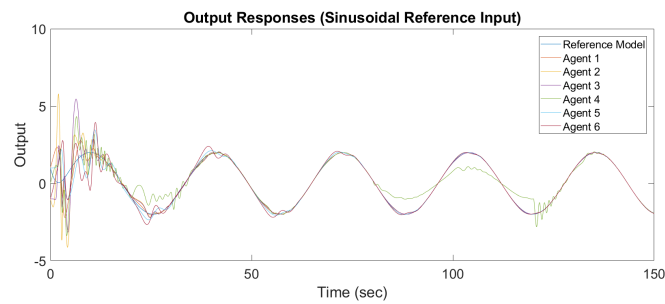


(a) Agent 4 without a switching controller

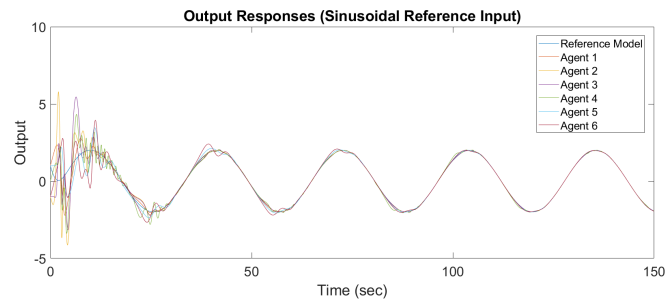


(b) Agent 4 with a switching controller

Figure 5-4: Output response of the output-feedback MRAC with a constant input reference where the controller is not switching (a) and the controller is switching (b).



(a) Agent 4 without a switching controller



(b) Agent 4 with a switching controller

Figure 5-5: Output response of the output-feedback MRAC with a sinusoidal input reference where the controller is not switching (a) and the controller is switching (b).

It can be observed in Figures 5-4a and 5-5a that the output of Agent 4 does not converge to the output of the leader, while in Figures 5-4b and 5-5b all the outputs converge asymptotically to the output of the leader. It can be concluded that, in the case of switching topologies, the switching adaptive controller must be implemented.

5-2 Cyclic state-feedback MRAC: Platooning merging maneuver

The platooning merging maneuver will be used as a numerical example of adaptive synchronization based on state-feedback MRAC. In this case, we have time-varying topologies and communication graph with a cycle. First, let us consider the model derived by [46] is used to represent the vehicles in the platoon

$$\begin{pmatrix} \dot{d}_i \\ \dot{v}_i \\ \dot{a}_i \end{pmatrix} = \begin{pmatrix} v_i \\ a_i \\ -\frac{1}{\tau_i}a_i + \frac{1}{\tau_i}u_i \end{pmatrix}, \quad i \in S_M \quad (5-5)$$

where a_i and u_i are respectively the acceleration (m/s^2) and external input (m/s^2) of the i^{th} vehicle. Moreover, τ_i (s) represents each vehicle's driveline time constant.

It is now possible to define the spacing error (m) between the j^{th} and the i^{th} vehicle as:

$$e_{ji}(t) = \begin{pmatrix} d_j(t) \\ v_j(t) \\ a_j(t) \end{pmatrix} - \begin{pmatrix} d_i(t) \\ v_i(t) \\ a_i(t) \end{pmatrix} + \begin{pmatrix} r_{ji}(t) \\ 0 \\ 0 \end{pmatrix} \quad (5-6)$$

where r_{ij} depends on time because it is allowed to change during the merging maneuver. Substituting (5-6) in (5-5) we obtain the linear time-invariant state space system

$$\begin{pmatrix} \dot{d}_i \\ \dot{v}_i \\ \dot{a}_i \end{pmatrix} = \underbrace{\begin{pmatrix} 0 & 1 & 0 \\ 0 & 0 & 1 \\ 0 & 0 & -\frac{1}{\tau_i} \end{pmatrix}}_{A_i} \underbrace{\begin{pmatrix} d_i \\ v_i \\ a_i \end{pmatrix}}_{x_i} + \underbrace{\begin{pmatrix} 0 \\ 0 \\ \frac{1}{\tau_i} \end{pmatrix}}_{b_i} u_i. \quad (5-7)$$

Furthermore, the leading vehicle's model is defined as

$$\begin{aligned} \begin{pmatrix} \dot{d}_0 \\ \dot{v}_0 \\ \dot{a}_0 \end{pmatrix} &= \begin{pmatrix} 0 & 1 & 0 \\ 0 & 0 & 1 \\ 0 & 0 & -\frac{1}{\tau_0} \end{pmatrix} \begin{pmatrix} d_0 \\ v_0 \\ a_0 \end{pmatrix} + \begin{pmatrix} 0 \\ 0 \\ \frac{1}{\tau_0} \end{pmatrix} u_0 \\ \begin{pmatrix} \dot{d}_0 \\ \dot{v}_0 \\ \dot{a}_0 \end{pmatrix} &= \underbrace{\begin{pmatrix} 0 & 1 & 0 \\ 0 & 0 & 1 \\ a_{01} & a_{02} & a_{03} \end{pmatrix}}_{A_m} \underbrace{\begin{pmatrix} d_0 \\ v_0 \\ a_0 \end{pmatrix}}_{x_m} + \underbrace{\begin{pmatrix} 0 \\ 0 \\ b_{00} \end{pmatrix}}_{b_m} r \end{aligned} \quad (5-8)$$

Fig. 5-6 shows the switching topologies for the merging maneuver. The merging maneuver starts with network 1, with a platoon consisting of vehicle 1 and vehicle 2: before attempting the merging maneuver, vehicle 3 aligns to vehicle 2. When the merging starts (network 2), a communication graph with a cycle appears (due to safety reasons an undirected edge between agent 2 and agent 3 is created): vehicle 2 increases its distance from vehicle 1, and vehicle 3 tries to stay in the middle of the two vehicles. The undirected edge between vehicle 2 and vehicle 3 is used by vehicle 2 to watch the behavior of vehicle 3 and vice versa (as it happens in merging maneuvers operated by humans). Finally, in network 3, the merging is complete and a new acyclic directed network is established between the three vehicles.

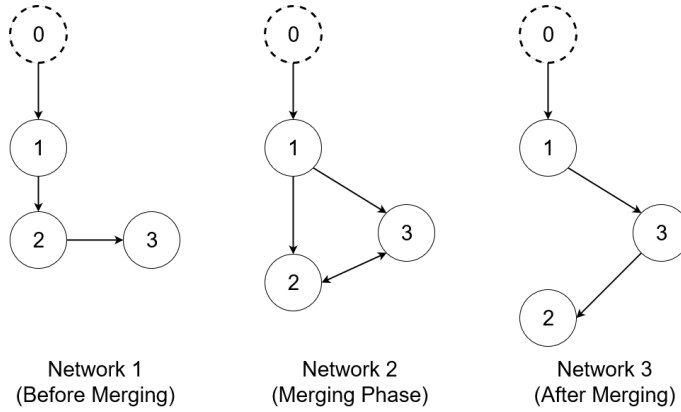


Figure 5-6: The communication graphs before, during and after merging (Platooning Merging Maneuver Case)

The following CDH spacing policies apply to the three networks:

- Network 1
 $r_{32} = 0$ and $r_{21} = \rho$ for a certain design parameter ρ ;
- Network 2
 r_{21} increases linearly from ρ to 2ρ , r_{32} decreases linearly from 0 to $-\rho$, and $r_{31} = \rho$;
- Network 3
 $r_{31} = \rho$ and $r_{23} = \rho$;

while $e_{10} = e_1 = x_1 - x_m$ for all three networks.

The parameters of the reference model are taken as: $a_{01} = -4$, $a_{02} = -6$, $a_{03} = -4$, and $b_{00} = 1$, while the dynamics of the vehicles in (5-7) are unknown. Table 5-2 shows the parameter for each vehicle i , together with their initial conditions. These parameters are used only to simulate the unknown heterogeneous agents.

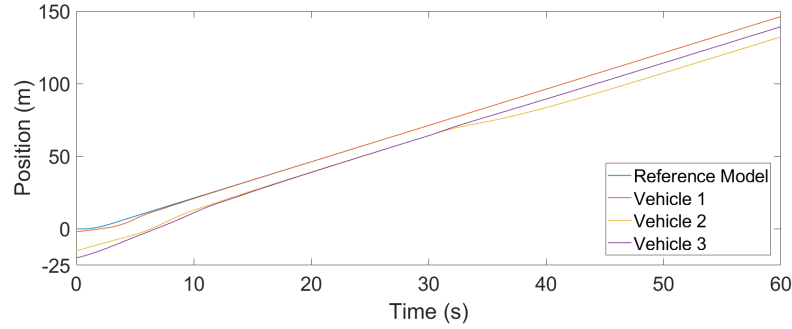
The reference signal r is taken to be a ramp. Please note that all the simulations are carried out at low speed (around 2.5m/s) so that the gaps between vehicles can

Table 5-2: Vehicles parameters and initial conditions

Vehicle i	τ_i	$x_i(0)$
Vehicle 0	-	$[0,0,0]$
Vehicle 1	0.5	$[-2,1,0]$
Vehicle 2	0.33	$[-15,2,1]$
Vehicle 3	0.2	$[-20,2,1]$

be better visualized in the plots. Please note that we have verified that the proposed approach would work also at higher speeds. The other design parameter are taken as: $Q = \text{diag}(1, 1, 5)$, $\rho = 7m$, the adaptive gains $\gamma_k = 0.005$, $\gamma_l = 0.001$, and all coupling gains, k_i , k_{ij} , l_i , l_{ij} , are initialized to 0. The merging maneuver is organized as follows

- 0-30 s: vehicle 3 aligns with vehicle 2, while vehicles 1 and 2 achieve the initial formation.
- 30-50s: vehicle 2 creates an increasing gap for vehicle 3, while vehicle 3 starts the merging.
- 50-60s: the final formation is achieved.

**Figure 5-7:** The position response (Platooning Merging Maneuver Case)

Figs. 5-7, 5-8, 5-9, and 5-10 show the response of p_i , v_i , a_i , and u_i , respectively. In Fig. 5-7, we can observe in the interval 0-30 seconds (network 1), the distance of vehicle 2 and vehicle 3 are at a distance ρ from vehicle 1, at the same time vehicle 1 synchronize to reference model. Then, in the interval 30-50 seconds (network 2), vehicle 2 makes a gap by increasing the distance with vehicle 1 in order to allow vehicle 3 to merge in between vehicle 1 and vehicle 2. Finally, in the interval 50-60 seconds (network 3), vehicle 3 is located at a distance ρ from vehicle 1 and vehicle 2 is located at a distance 2ρ from vehicle 1.

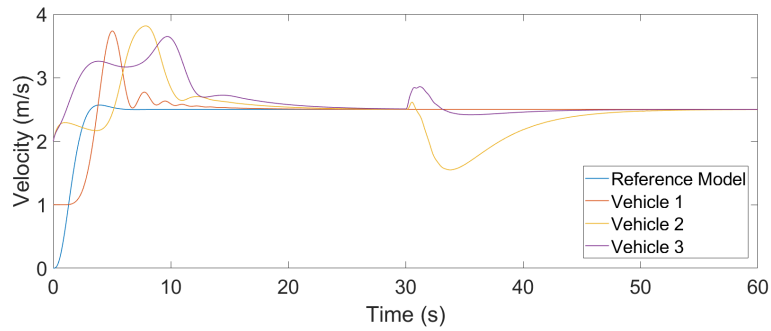


Figure 5-8: The velocity response (Platooning Merging Maneuver Case)

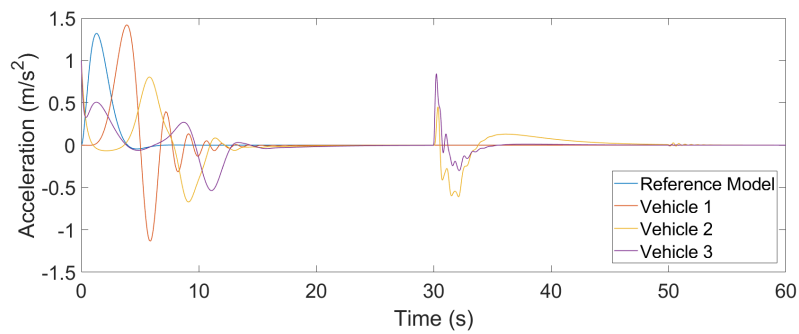


Figure 5-9: The acceleration response (Platooning Merging Maneuver Case)

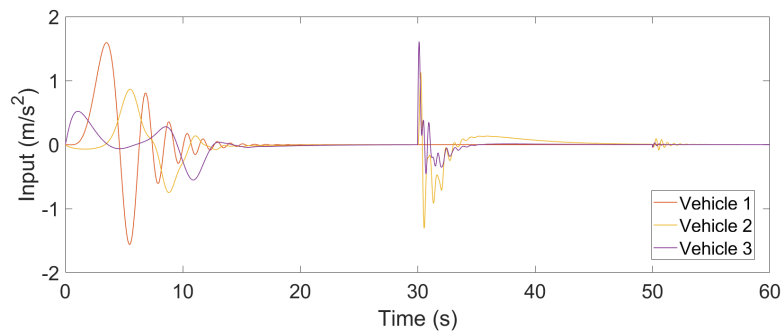


Figure 5-10: The input response (Platooning Merging Maneuver Case)

5-3 Euler-Lagrange systems MRAC: Formation control for multi-aircraft systems

Simulations are performed using the following reference model dynamics and parameters:

$$A_m = \begin{bmatrix} 0 & \mathbb{1} \\ -k_p \mathbb{1} & -k_v \mathbb{1} \end{bmatrix} \quad B_m = \begin{bmatrix} 0 \\ \mathbb{1} \end{bmatrix} \quad r = \begin{bmatrix} k_p x^d + k_v \dot{x}^d + \ddot{x}^d \\ k_p y^d + k_v \dot{y}^d + \ddot{y}^d \\ k_p z^d + k_v \dot{z}^d + \ddot{z}^d \\ k_p \phi^d + k_v \dot{\phi}^d + \ddot{\phi}^d \\ k_p \theta^d + k_v \dot{\theta}^d + \ddot{\theta}^d \\ k_p \psi^d + k_v \dot{\psi}^d + \ddot{\psi}^d \end{bmatrix} \quad (5-9)$$

$$Q = 100\mathbb{1} \quad k_p = 50 \quad k_v = 50 \quad S_1 = \dots = S_4 = 100\mathbb{1}$$

where, for each agent j , the state is $x_j = [q_j' \quad \dot{q}_j']'$, being q_j the generalized UAV coordinates in the body frame. In addition, q^d , \dot{q}^d , and \ddot{q}^d are obtained from an UAV flying in a windy environment and implementing a vector field approach as in [47]: this UAV represents the pinner UAV. We consider constant airspeed $V_a = 15 \text{ m/s}$, constant altitude $h_m = 50 \text{ m}$, and slowly-varying wind with amplitude $A(t) = 3\sin(0.01t)$ and slowly-varying wind angle $\psi_w(t) = \pi\sin(0.01t)$. The control parameters of the vector field approach are $\kappa = \frac{\pi}{2}$, $k = 0.1$, $\epsilon = 1$, $\Gamma = 0.1$, and $\sigma = 0$, whose exact meaning can be retrieved from [47].

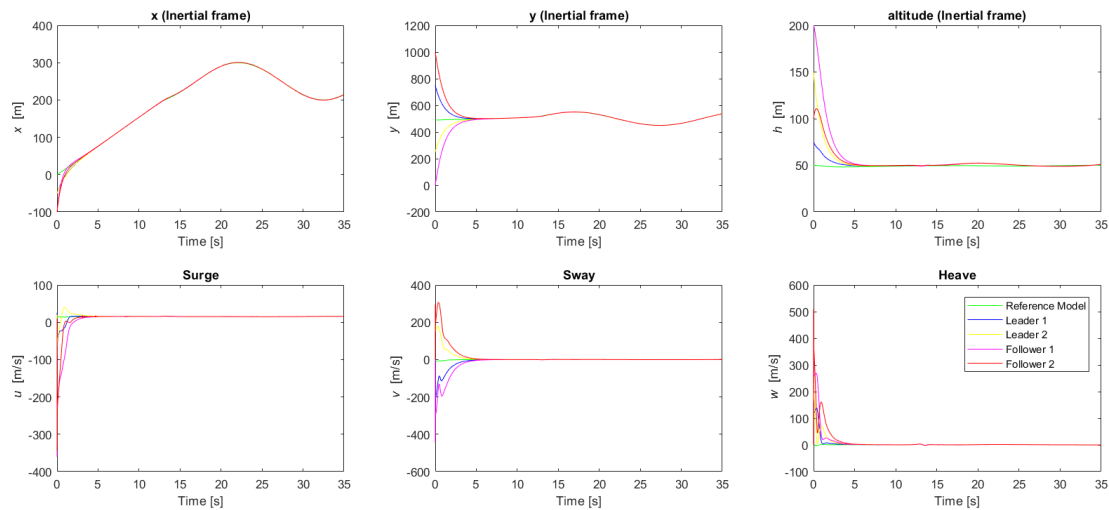
In line with most UAV path generation approaches, the path is composed of straight lines and orbits. For these simulations we take a path consisting of a straight line followed an orbit with radius $R = 50 \text{ m}$ and orbit center $c = [500 \text{ m}, 250 \text{ m}]$. The simulations of the multi-UAV formation are carried out for 4 UAVs and a pinner UAV under the same communication graph shown in Figure 1. Table 5-3 shows the parameters of the fixed-wing UAVs, which are used only for the sake of simulations and are unknown for the purpose of control design.

Figures 5-11 and 5-12 show the state synchronization for all UAVs, where it is immediate to see that all states converge to the reference model. The states are reported in the inertial frame for an easier interpretation of the results. Figure 5-13 shows how the UAVs behave in the inertial \mathbf{xy} plane. It can be seen that by synchronizing to the reference model, all the agents perform the path consisting of the straight line and the orbit.

Clearly, in Figure 5-13, the UAVs converge to the same point (rendezvous) due to the fact that we did not implement any desired formation (no formation gaps). In order to do so, we provide the desired gaps among agents, in such a way to describe a V formation. For convenience, we introduce first the gaps \bar{d}_{ji}^e in the inertial frame: \bar{d}_{10}^e , $\bar{d}_{21}^e = [50, -100, 0, 0, 0, 0]$, and $\bar{d}_{30}^e, \bar{d}_{43}^e = [50, 100, 0, 0, 0, 0]$. These gaps describe the V formation: obviously, it is possible to introduce more complex gaps in the $\mathbf{x}, \mathbf{y}, \mathbf{z}$ space

Table 5-3: Fixed-wing UAVs parameters and initial conditions

	Mass (kg)	Initial cond. $[x, y, z, \phi, \theta, \psi]'(0)$	Initial cond. $[\bar{u}, \bar{v}, \bar{w}, \bar{p}, \bar{q}, \bar{r}]'(0)$	Moment of Inertia (kg m ²)
Agent 0 (Trajectory Generator)	10	$[-50, 500, -50, 0, 0, 0]'$	$[15, 0, 0, 0, 0, 0]'$	$\begin{bmatrix} 0.02 & 0 & -0.01 \\ 0 & 0.026 & 0 \\ -0.01 & 0 & 0.053 \end{bmatrix}$
Agent 1 (Leader 1)	20	$[-50, 750, -75, 0.5, 0.05, 0.5]'$	$[25, 0, 0, 0, 0, 0]'$	$\begin{bmatrix} 0.1 & 0 & -0.01 \\ 0 & 0.05 & 0 \\ -0.01 & 0 & 0.1 \end{bmatrix}$
Agent 2 (Follower 1)	30	$[-100, -1000, -100, 1, 0.1, 1]'$	$[5, 0, 0, 0, 0, 0]'$	$\begin{bmatrix} 0.2 & 0 & -0.02 \\ 0 & 0.1 & 0 \\ -0.02 & 0 & 0.2 \end{bmatrix}$
Agent 3 (Leader 2)	40	$[-50, 250, -150, -0.5, -0.05, -0.5]'$	$[20, 0, 0, 0, 0, 0]'$	$\begin{bmatrix} 0.4 & 0 & -0.04 \\ 0 & 0.2 & 0 \\ -0.04 & 0 & 0.4 \end{bmatrix}$
Agent 4 (Follower 2)	50	$[-100, 0, -200, -1, -0.1, -1]'$	$[10, 0, 0, 0, 0, 0]'$	$\begin{bmatrix} 0.8 & 0 & -0.08 \\ 0 & 0.4 & 0 \\ -0.08 & 0 & 0.8 \end{bmatrix}$

**Figure 5-11:** Adaptive state synchronization for states $(x, y, z, \bar{u}, \bar{v}, \bar{w})$ (Synchronization of Multi-Aircraft System)

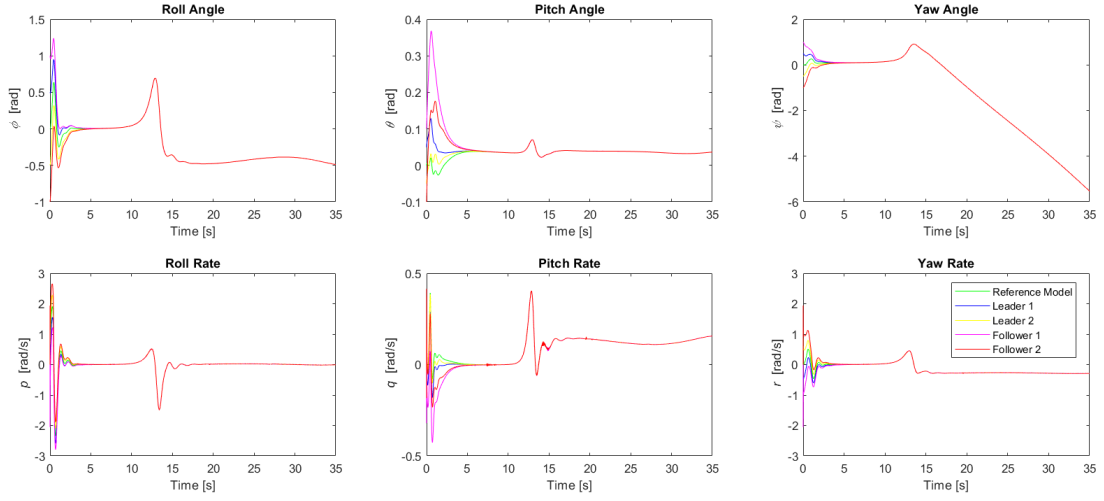


Figure 5-12: Adaptive state synchronization for states $(\phi, \theta, \psi, \bar{p}, \bar{q}, \bar{r})$ (Synchronization of Multi-Aircraft System)

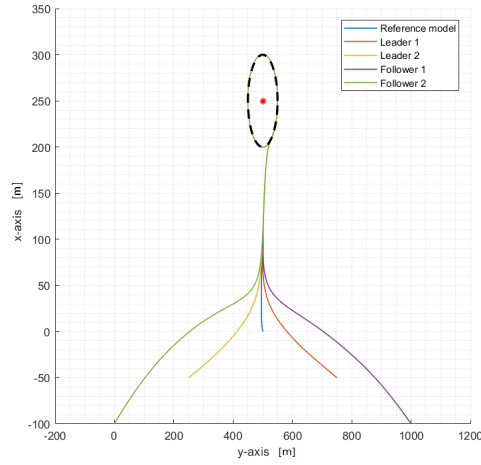


Figure 5-13: Adaptive state synchronization in the inertial xy plane without formation gaps (Synchronization of Multi-Aircraft System)

to perform more complicated flight formations. The error e_{ji}^e in inertial frame is

$$e_{ji}^e = x_j^e - x_i^e + \bar{d}_{ji}^e. \quad (5-10)$$

Then, we translate the error to the body frame by introducing the rotation matrix \mathcal{R}

$$e_{ji} = \mathcal{R}e_{ji}^e \quad (5-11)$$

where

$$\mathcal{R}(\phi, \theta, \psi) = \begin{bmatrix} \cos\theta\cos\psi & \cos\theta\sin\psi & -\sin\theta \\ -\cos\phi\sin\psi + \sin\phi\sin\theta\cos\psi & \cos\phi\cos\psi + \sin\phi\sin\theta\sin\psi & \sin\phi\cos\theta \\ \sin\phi\sin\psi + \cos\phi\sin\theta\cos\psi & -\sin\phi\cos\psi + \cos\phi\sin\theta\sin\psi & \cos\phi\cos\theta \end{bmatrix} \quad (5-12)$$

so as to implement control and adaptive laws in the body frame. Figure 5-14 shows, in the inertial xy plane, that the V-formation of fixed wing UAVs can be achieved, which demonstrates the effectiveness of the proposed adaptive formation algorithm.

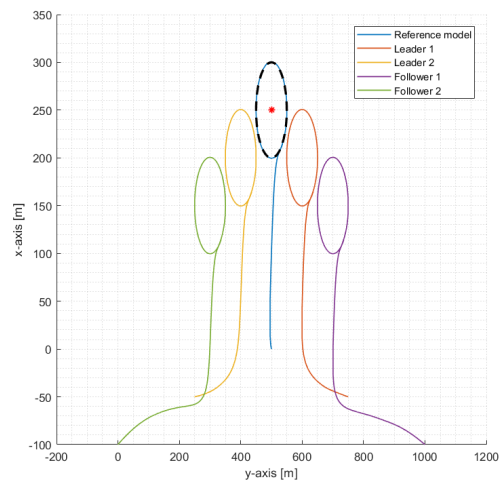


Figure 5-14: Adaptive formation control in the inertial xy plane for V formation flight (Synchronization of Multi-Aircraft System)

Conclusion and future work

6-1 Conclusion

In this work, it was shown that the output synchronization of a heterogeneous MASs with unknown dynamics can be achieved through extended version of output-feedback MRAC. In contrast with standard MRAC, where the adaptive gain is scalar-valued, in this proposed approach, the adaptive gain is a diagonal matrix. By using the proposed control law, the agents only require the output and the control input of its neighbors. The effectiveness of the proposed methodology has been illustrated using multi-UAV attitude control. Then, we have shown that it is possible to exploit the graph structure to implement appropriate parameter projection and guarantee well-posedness of the actual inputs. The effectiveness of the proposed methodology has been illustrated by using a platoon of three vehicles during merging maneuver. Finally, this work has shown the possibility to synchronize uncertain heterogeneous agents with Euler-Lagrange dynamics. A distributed model reference adaptive control is used to synchronize the Euler-Lagrange systems, which utilizes local states and input information, without any extra auxiliary variables nor sliding modes. The effectiveness of the proposed methodology has been verified via numerical simulations of a formation of Unmanned Aerial Vehicles.

In our proposed approaches, the presence of uncertainty is handled first by showing that distributed matching gains exist between neighboring agents, and then by developing adaptive laws to estimate these gains. Such distributed matching conditions and adaptive laws allow all agents to converge to same homogeneous reference model dynamics and thus synchronize. The stabilities of the proposed controllers have derived analytically by introducing an appropriately defined distributed Lyapunov function.

6-2 Future work

Future work will consider the presence of under-actuated Euler-Lagrange dynamics where a control allocator technique should be introduced to transform the input, forces and moments, into the actual input to the system i.e. for fixed-wing UAV we have aileron deflection, rudder deflection, elevator deflection, and propeller thrust. In the simulations, it has been shown that the switching topologies could be handled by introducing the switching controller. However, the stability proof is an open problem and might be proven using the adaptive switched tools [26, 27]. Future work could include the possibility to handle non-hierarchical networks of Euler-Lagrange systems. Another interesting problem is how to deal with networked-induced constraints. In [39] it is shown that communication losses can be possibly managed. Similarly, we believe that limited communication, e.g. quantization can be handled in line with [48]. Another relevant direction is, in line with [49, 50], to consider practical constraints such as input constraints and actuator saturation. Finally, in the implementation, capabilities such as obstacle-avoidance and collision-avoidance is necessary.

Bibliography

- [1] W. Yu, G. Chen, and J. Lu, “On pinning synchronization of complex dynamical networks,” *Automatica*, vol. 45, no. 2, pp. 429 – 435, 2009.
- [2] W. Yu, P. DeLellis, G. Chen, M. di Bernardo, and J. Kurths, “Distributed adaptive control of synchronization in complex networks,” *IEEE Transactions on Automatic Control*, vol. 57, no. 8, pp. 2153–2158, 2012.
- [3] W. Ren, R. W. Beard, and A. W. Beard, “Decentralized scheme for spacecraft formation flying via the virtual structure approach,” *AIAA Journal of Guidance, Control, and Dynamics*, vol. 27, pp. 73–82, 2003.
- [4] V. Lesser, M. Tambe, and C. L. Ortiz, eds., *Distributed Sensor Networks: A Multiagent Perspective*. Norwell, MA, USA: Kluwer Academic Publishers, 2003.
- [5] I. T. Michailidis, T. Schild, R. Sangi, P. Michailidis, C. Korkas, J. Futterer, D. Muller, and E. B. Kosmatopoulos, “Energy-efficient HVAC management using cooperative, self-trained, control agents: A real-life German building case study,” *Applied Energy*, vol. 211, pp. 113 – 125, 2018.
- [6] G. Wen, X. Yu, Z. W. Liu, and W. Yu, “Adaptive consensus-based robust strategy for economic dispatch of smart grids subject to communication uncertainties,” *IEEE Transactions on Industrial Informatics*, vol. 14, no. 6, pp. 2484–2496, 2018.
- [7] I. A. Azzollini, S. Baldi, and E. B. Kosmatopoulos, “Adaptive synchronization in networks with heterogeneous uncertain kuramoto-like units,” *2018 European Control Conference*, 2018.
- [8] M. Jun and R. D’Andrea, *Path Planning for Unmanned Aerial Vehicles in Uncertain and Adversarial Environments*, pp. 95–110. Boston, MA: Springer US, 2003.

- [9] B. Grocholsky, J. Keller, V. Kumar, and G. Pappas, "Cooperative air and ground surveillance," *IEEE Robotics Automation Magazine*, vol. 13, no. 3, pp. 16–25, 2006.
- [10] D. O. Popa, A. C. Sanderson, R. J. Komerska, S. S. Mupparapu, D. R. Blidberg, and S. G. Chappel, "Adaptive sampling algorithms for multiple autonomous underwater vehicles," in *2004 IEEE/OES Autonomous Underwater Vehicles*, pp. 108–118, 2004.
- [11] G. Weiss, ed., *Multiagent Systems: A Modern Approach to Distributed Artificial Intelligence*. Cambridge, MA, USA: MIT Press, 1999.
- [12] R. Walter, Brenner Zarnekow and W. H., *Intelligent software agents foundations and applications*. Springer Science and Business Media, 2012.
- [13] P. Frasca, R. Carli, F. Fagnani, and S. Zampieri, "Average consensus on networks with quantized communication," *International Journal of Robust and Nonlinear Control*, vol. 19, no. 16, pp. 1787–1816.
- [14] L. Zhang, H. Gao, and O. Kaynak, "Network-induced constraints in networked control systems. a survey," *IEEE Transactions on Industrial Informatics*, vol. 9, no. 1, pp. 403–416, 2013.
- [15] S. He, G. Yi, and Z. Wu, "Exponential synchronization of dynamical network with distributed delays via intermittent control," *Asian Journal of Control*, vol. 0, no. 0.
- [16] Y. Cao, W. Yu, W. Ren, and G. Chen, "An overview of recent progress in the study of distributed multi-agent coordination," *IEEE Transactions on Industrial Informatics*, vol. 9, no. 1, pp. 427–438, 2013.
- [17] W. Ren and R. W. Beard, "A decentralized scheme for spacecraft formation flying via the virtual structure approach," in *Proceedings of the 2003 American Control Conference.*, vol. 2, pp. 1746–1751, June 2003.
- [18] M. Zhang, A. Saberi, and A. A. Stoorvogel, "Synchronization for a network of identical discrete-time agents with unknown, nonuniform constant input delay," in *2015 54th IEEE Conference on Decision and Control (CDC)*, pp. 7054–7059, Dec 2015.
- [19] F. Dorfler and F. Bullo, "Synchronization in complex networks of phase oscillators: A survey," *Automatica*, vol. 50, no. 6, pp. 1539 – 1564, 2014.
- [20] M. Zhang, A. Saberi, H. F. Grip, and A. A. Stoorvogel, " h_∞ almost output synchronization for heterogeneous networks without exchange of controller states," *IEEE Transactions on Control of Network Systems*, vol. 2, pp. 348–357, Dec 2015.
- [21] Z. Li, Z. Duan, and F. L. Lewis, "Distributed robust consensus control of multi-agent systems with heterogeneous matching uncertainties," *Automatica*, vol. 50, no. 3, pp. 883 – 889, 2014.

-
- [22] G. S. Seyboth, W. Ren, and F. Allgower, “Cooperative control of linear multi-agent systems via distributed output regulation and transient synchronization,” *Automatica*, vol. 68, no. Supplement C, pp. 132 – 139, 2016.
 - [23] S. Baldi, “Cooperative output regulation of heterogeneous unknown systems via passification-based adaptation,” *IEEE Control Systems Letters*, vol. 2, pp. 151–156, Jan 2018.
 - [24] S. Baldi, I. A. Azzollini, and E. B. Kosmatopoulos, “A distributed disagreement-based protocol for synchronization of uncertain heterogeneous agents,” *2018 European Control Conference*, 2018.
 - [25] S. Baldi and P. Frasca, “Adaptive synchronization of unknown heterogeneous agents: An adaptive virtual model reference approach,” *Journal of the Franklin Institute*, 2018.
 - [26] S. Yuan, B. De Schutter, and S. Baldi, “Robust adaptive tracking control of uncertain slowly switched linear systems,” *Nonlinear Analysis: Hybrid Systems*, vol. 27, no. Supplement C, pp. 1 – 12, 2018.
 - [27] S. Yuan, B. De Schutter, and S. Baldi, “Adaptive asymptotic tracking control of uncertain time-driven switched linear systems,” *IEEE Transactions on Automatic Control*, vol. 62, pp. 5802–5807, Nov 2017.
 - [28] W. Wang, C. Wen, J. Huang, and Z. Li, “Hierarchical decomposition based consensus tracking for uncertain interconnected systems via distributed adaptive output feedback control,” *IEEE Transactions on Automatic Control*, vol. 61, pp. 1938–1945, July 2016.
 - [29] S. Baldi, S. Yuan, and P. Frasca, “Output synchronization of unknown heterogeneous agents via distributed model reference adaptation,” *IEEE Transactions on Control of Network Systems*, pp. 1–1, 2018.
 - [30] P. A. Ioannou and B. Fidan, *Adaptive control tutorial*. Society for Industrial and Applied Mathematics Philadelphia, Pa, 2006.
 - [31] M. R. Rosa, “Adaptive synchronization for heterogeneous multi-agent systems with switching topologies,” *Machines MDPI*, vol. 6, 2018.
 - [32] P. A. Ioannou and J. Sun, *Robust Adaptive Control*. Upper Saddle River, NJ, USA: Prentice-Hall, Inc., 1995.
 - [33] R. Ortega and M. W. Spong, “Adaptive motion control of rigid robots: a tutorial,” in *Proceedings of the 27th IEEE Conference on Decision and Control*, pp. 1575–1584 vol.2, 1988.
 - [34] G. Tao, *Adaptive Control Design and Analysis (Adaptive and Learning Systems for Signal Processing, Communications and Control Series)*. New York, NY, USA: John Wiley & Sons, Inc., 2003.

- [35] P. Ioannou and B. Fidan, *Adaptive Control Tutorial (Advances in Design and Control)*. Philadelphia, PA, USA: Society for Industrial and Applied Mathematics, 2006.
- [36] G. Tao, "Multivariable adaptive control: A survey," *Automatica*, vol. 50, no. 11, pp. 2737 – 2764, 2014.
- [37] S. Ghapani, J. Mei, W. Ren, and Y. Song, "Fully distributed flocking with a moving leader for lagrange networks with parametric uncertainties," *Automatica*, vol. 67, pp. 67 – 76, 2016.
- [38] H. Cai and J. Huang, "The leader-following consensus for multiple uncertain Euler-Lagrange systems with an adaptive distributed observer," *IEEE Transactions on Automatic Control*, vol. 61, no. 10, pp. 3152–3157, 2016.
- [39] Y. A. Harfouch, S. Yuan, and S. Baldi, "An adaptive approach to cooperative longitudinal platooning of heterogeneous vehicles with communication losses," *IFAC-PapersOnLine*, vol. 50, no. 1, pp. 1352 – 1357, 2017. 20th IFAC World Congress.
- [40] Y. A. Harfouch, S. Yuan, and S. Baldi, "An adaptive switched control approach to heterogeneous platooning with inter-vehicle communication losses," *IEEE Transactions on Control of Network Systems*, pp. 1–1, 2017.
- [41] S. Baldi, G. Battistelli, E. Mosca, and P. Tesi, "Multi-model unfalsified adaptive switching supervisory control," *Automatica*, vol. 46, no. 2, pp. 249 – 259, 2010.
- [42] J. P. Hespanha, D. Liberzon, and A. Morse, "Hysteresis-based switching algorithms for supervisory control of uncertain systems," *Automatica*, vol. 39, no. 2, pp. 263 – 272, 2003.
- [43] K. S. Narendra and J. Balakrishnan, "Adaptive control using multiple models," *IEEE Transactions on Automatic Control*, vol. 42, pp. 171–187, Feb 1997.
- [44] F. Nex and F. Remondino, "Uav for 3d mapping applications: a review," *Applied Geomatics*, vol. 6, pp. 1–15, Mar 2014.
- [45] S. I. Tomashevich, A. L. Fradkov, B. Andrievsky, A. O. Belyavskiy, and K. Amelin, "Simple adaptive control of quadrotor attitude. algorithms and experimental results," in *2017 25th Mediterranean Conference on Control and Automation (MED)*, pp. 933–938, July 2017.
- [46] J. Ploeg, N. van de Wouw, and H. Nijmeijer, "Lp string stability of cascaded systems: Application to vehicle platooning," *IEEE Transactions on Control Systems Technology*, vol. 22, pp. 786–793, March 2014.
- [47] B. Zhou, H. Satyavada, and S. Baldi, "Adaptive path following for unmanned aerial vehicles in time-varying unknown wind environments," in *2017 American Control Conference (ACC)*, pp. 1127–1132, 2017.

-
- [48] N. Moustakis, S. Yuan, and S. Baldi, “An adaptive design for quantized feedback control of uncertain switched linear systems,” *International Journal of Adaptive Control and Signal Processing*, vol. 32, pp. 664 – 680, 2018.
 - [49] E. Lavretsky and N. Hovakimyan, “Stable adaptation in the presence of input constraints,” *Systems and Control Letters*, vol. 56, no. 11, pp. 722 – 729, 2007.
 - [50] S. Yuan, L. Zhang, O. Holub, and S. Baldi, “Switched adaptive control of air handling units with discrete and saturated actuators,” *IEEE Control Systems Letters*, vol. 2, no. 3, pp. 417–422, 2018.

